

Forcing, damping and detuning for single and coupled van der Pol oscillators

D. R. J. Chillingworth* Z. Afshar-nejad†

February 27, 2013

Abstract

We use Melnikov function techniques together with geometric methods of bifurcation theory to study the interactions of forcing, damping and detuning on resonant periodic orbits for single and coupled forced van der Pol oscillators. For a coupled pair the local bifurcation geometry is almost everywhere described in terms of the singularities of a line congruence in three dimensions.

1 Introduction

The search for harmonic and subharmonic periodic orbits of a single or several coupled forced nonlinear oscillators such as the van der Pol system

$$\begin{aligned} \dot{x} &= \omega_0 y \\ \dot{y} &= -\omega_0 x - \delta(x^2 - 1)y + \varepsilon \cos(\omega t) \end{aligned} \tag{1.1}$$

(here $x, y \in \mathbf{R}$ while δ, ε are small constants and the angular frequency ω of the forcing term is close to the natural frequency ω_0 of the linear system) has a long and distinguished pedigree, originating in mechanical and electrical engineering and more recently of major interest in the biological sciences with particular reference to *synchronisation*: see for example [4],[6],[21],[24],[28],[29]. We do not attempt to survey here the vast literature on forced or coupled

*Mathematics, University of Southampton, Southampton SO17 1BJ, UK (drjc@maths.soton.ac.uk).

†Applied Mathematics Department, Ferdowsi University of Mashhad, Iran (afsharnejad@math.um.ac.ir).

oscillators, but refer to standard texts such as [13, 25, 26] for classical background or [12, Ch.11],[19, Ch.4] for more recent approaches.

From the geometrical dynamics point of view the natural object of study for a system of m weakly coupled oscillators each having an attracting limit cycle is an m -dimensional invariant torus (the cartesian product of the limit cycles) on which the flow is periodic or quasiperiodic, depending on the rational relations or otherwise between the frequencies of the component oscillators. On a cross-section of the flow the dynamics is modelled by a discrete dynamical system (Poincaré map) on a torus of dimension $m - 1$, this system being close to the direct product of $m - 1$ rigid rotations. For $m = 2$ the creation and annihilation of periodic orbits of various periods on the circle (1-dimensional torus) in response to perturbations of frequency and amplitude is typically described by *Arnold tongues* [3, Ch.3,§11], while for $m = 3$ the situation naturally becomes much more complicated [5],[15],[28].

In the present setting (1.1) we begin not with a limit cycle or cycles (on which after forcing or coupling perturbations the above remarks apply), but with a linear system of simple harmonic motion in the plane which, as is well known (see e.g. [25]) gives rise to a limit cycle of variable amplitude when a nonlinear van der Pol damping perturbation (the δ -term in (1.1)) is introduced. At the same time an independent small-amplitude forcing term $\varepsilon \cos \omega t$ is applied with frequency close to but possibly detuned from that of the linear system. For ε small relative to δ the bifurcation is dominated by the limit cycle of the unforced van der Pol system and for small detuning as the forcing amplitude ε increases we see the creation of a pair of near-harmonic ((1 : 1) resonant) periodic solutions governed by an Arnold tongue as expected. This analysis can be found in standard texts such as [12, Ch.11] or [13, Ch.14, Th.3.1].

However, the original equilibrium state at the origin also persists as a near-harmonic periodic orbit (the so-called quasi-static solution) for the perturbed system. As detuning and forcing amplitude increase these periodic orbits interact and our bifurcation analysis (see Section 3 below) shows that the Arnold tongue splits into two, while across the ‘inside’ edges one of the orbits created within the tongue coalesces with the quasi-static orbit at a saddle-node bifurcation. As detuning increases further the tongues disappear at what turns out to be a cusp bifurcation point controlling the interaction of all three near-harmonic orbits. The bifurcation diagram is shown in Figure 3.2, where the coordinates a, α essentially represent the reciprocal of the detuning parameter and the forcing amplitude respectively: we refer to Section 3 for details.

Bifurcation results for systems of this general kind have been much studied in the literature, from various points of view. For example, conditions on the function g (assumed 2π -periodic in t) for the existence of 2π -periodic solutions to a system of the form

$$\ddot{x} + x = \varepsilon g(x, \dot{x}, t; \varepsilon)$$

for $x \in \mathbf{R}$ and small $\varepsilon \in \mathbf{R}$ can be found in [12] or [13]. See also [16] for an extension of the methods to include certain degeneracies, and also [23] for a quite different topological approach using index theory. In all cases the criteria involve integrating a certain function obtained from g around periodic solutions of the unperturbed equation, often called a Melnikov integral.

The main aim of this paper is to extend the theory of the Melnikov integral method, specifically as refined and developed in a series of papers by Chicone [7, 8, 9, 10], to a general multi-parameter setting, and then to illustrate the method by applying it first to a single and then to a coupled pair of van der Pol oscillators subject to forcing and detuning. The latter system is studied in [8], for example, but the bifurcation results are there described in terms of a single Melnikov (integral) bifurcation problem obtained after temporarily fixing the values of all parameters except one. In contrast, in the multiparameter setting developed in the present paper the bifurcations are seen to be controlled not by the vanishing of a single bifurcation (Melnikov) function but by the loss of rank of a bifurcation *matrix*. The kernel of this matrix determines to a first approximation the direction from the origin in parameter space along which bifurcations can occur.

These methods fit in to the general framework of multi-parameter bifurcation from a manifold as described in [11], and take their inspiration from Chicone's results as well as from earlier work of Hale and Taboas [20] on the interaction of forcing and damping for nonlinear oscillators. We believe our approach is not only a natural one from the geometric point of view but gives clearer insight into the relative roles of the key parameters than might be obtained by more analytical methods. We now describe the general technique in more detail.

1.1 Outline of the method

Let γ be a periodic orbit of period $T > 0$ for an autonomous system of ordinary differential equations

$$\dot{x} = f(x) \tag{1.2}$$

in \mathbf{R}^n , assuming sufficiently regularity so that solutions with given initial data are unique and are defined for all $t \in \mathbf{R}$. Then each point of γ is a fixed point for the map $\phi_T : \mathbf{R}^n \rightarrow \mathbf{R}^n$ where $\{\phi_t\}$ is the flow generated by the solutions of the equations. If we now perturb the system by applying a small-amplitude forcing of period T' close to T , while possibly at the same time amending the original equations slightly through the introduction of damping, for example, then the map

$$F : \mathbf{R}^n \rightarrow \mathbf{R}^n$$

defined by following solutions of the nonautonomous perturbed system for time T' is close to the original map ϕ_T . The problem of finding T' -periodic orbits of the perturbed system close to γ then becomes the problem of finding the fixed points (if any) ξ of F that are close to γ or, to express it another way, to find which points ξ_0 of γ *persist* nearby as periodic points ξ with period T' for the nonautonomous perturbed system. We call the corresponding T' -periodic orbit of ξ under the perturbed flow a *near-harmonic* periodic orbit emanating from ξ_0 .

1.1.1 A single perturbation parameter

A standard technique, which presumably goes back at least to Poincaré, is to consider the perturbation of (1.2) as depending on a single parameter $\varepsilon \in \mathbf{R}$ (with no perturbation when $\varepsilon = 0$) and, given sufficient smoothness, to expand the corresponding map $F = F_\varepsilon$ in powers of ε on a neighbourhood U of γ . The *displacement map*, that is the difference

$$P_\varepsilon = F_\varepsilon - id$$

between F_ε and the identity map, vanishes at least on γ when $\varepsilon = 0$, but may vanish on a larger set: indeed, in a wide class of examples (including ours) in which $n = 2$ and the unperturbed system is a simple harmonic oscillator, the map P_0 vanishes on the whole of \mathbf{R}^2 . Let $V \subset U$ denote the zero set of P_0 . Then at points $x \in V$ the expansion of F_ε in powers of ε has ε as a factor. After removal of this factor, the remaining term without ε is the first derivative

$$P' := \left. \frac{\partial P_\varepsilon}{\partial \varepsilon} \right|_{\varepsilon=0} : V \rightarrow \mathbf{R}^n, \quad (1.3)$$

called the *bifurcation map*. If $P'(\xi) \neq 0$ there there can be no zeros of P_ε close to ξ when $|\varepsilon|$ is sufficiently small. We state this as the first key result.

Proposition 1.1 *A necessary condition for a branch of near-harmonic periodic orbits to emanate from $\xi_0 \in V$ as ε moves away from zero is that $P'(\xi_0) = 0$. \square*

Finally, by the implicit function theorem (IFT), provided the zeros of P' are nondegenerate (the Jacobian matrix of P' there is nonsingular), these zeros will persist nearby as zeros of P_ε for small $\varepsilon \neq 0$, and correspond to periodic orbits of the perturbed system with period T' .

This method is effective for a single parameter as long as the zeros of P' are nondegenerate, but further questions arise if P' has zeros that are degenerate. A class of ODE problems where this happens is studied for example by Hale and Taboas [20]: see also [12]. However, the philosophy of *unfolding* theory for singularities of smooth (that is, C^∞) maps and vector fields [2, 30] shows that the introduction of further parameters often enables degeneracies to be controlled and local bifurcation behaviour to be understood in a wider framework. This is the approach we exploit in this paper.

1.1.2 Multiple parameters

For a system as above but with perturbations depending on d parameters $\varepsilon = (\varepsilon_1, \dots, \varepsilon_d) \in \mathbf{R}^d$ we have for each $i = 1, \dots, d$ a bifurcation map as in (1.3)

$$P'_i : V \rightarrow \mathbf{R}^n,$$

obtained by setting all other parameters ε_j with $j \neq i$ equal to zero. We then assemble the $\{P'_i\}$ to form a map \mathcal{P} from V to the space $\mathcal{L}(d, n)$ of $n \times d$ real matrices.

Definition 1.2 *The bifurcation matrix $\mathcal{P}(\xi)$ is the $n \times d$ matrix whose i^{th} column is $P'_i(\xi) \in \mathbf{R}^n$ for $i = 1, \dots, d$. The map $\mathcal{P} : V \rightarrow \mathcal{L}(d, n)$ is called the bifurcation map for the perturbed system.*

With the displacement map $P_\varepsilon = F_\varepsilon - id : U \rightarrow \mathbf{R}^n$ defined as before but now with $\varepsilon \in \mathbf{R}^d$ we have

$$P_\varepsilon(\xi) = \mathcal{P}(\xi)\varepsilon + O(|\varepsilon|^2). \quad (1.4)$$

Taking polar coordinates in \mathbf{R}^d by writing $\varepsilon = \rho s$ where $\rho > 0$ and s belongs to the unit sphere S^{d-1} in \mathbf{R}^d , the expression (1.4) becomes

$$P_\varepsilon(\xi) = \rho \mathcal{P}(\xi)s + O(\rho^2) \quad (1.5)$$

from which it is clear that if $s_0 \notin \ker \mathcal{P}(\xi_0)$ then for sufficiently small $\rho > 0$ there are no solutions to $P_\varepsilon(\xi) = 0$ for any ξ in a neighbourhood of ξ_0 and any ε in a cone about the s_0 -axis in \mathbf{R}^d . Hence we are able to state the following result:

Proposition 1.3 *A necessary condition for a branch of near-harmonic periodic orbits to emanate from $\xi_0 \in V$ as ε moves away from the origin in \mathbf{R}^d in the direction of $s_0 \in S^{d-1}$ is that $s_0 \in \ker \mathcal{P}(\xi_0)$. \square*

That this necessary condition is not sufficient will become clear from examples that we consider below. However, the condition is sufficient if $s_0 \in \ker \mathcal{P}(\xi_0)$ in a way which is nondegenerate with respect to the family of kernels $\{\ker \mathcal{P}(\xi)\}$ as ξ varies near ξ_0 . The precise meaning of this statement varies depending on the relative sizes of n and d , and we refer to [11] for a fuller discussion of this issue.

In the case of a single forced van der Pol system we shall be concerned with $n = d = 2$. Here, a typical 2×2 matrix is nonsingular and so has zero kernel, and it is a codimension-1 occurrence for the matrix to have kernel of dimension 1. This is the geometry we exploit in order to locate near-harmonic periodic orbits for the system (1.1).

For a coupled pair of van der Pol systems in Section 4 we focus instead on the 2-dimensional kernels of a family of 4×4 matrices. The intersections of these kernels with the unit sphere S^3 in \mathbf{R}^4 projects stereographically to a 2-parameter family of lines (or *line congruence*) in \mathbf{R}^3 and local bifurcation geometry is generically determined by the local structure of this line congruence. We are not able to present a complete analysis in this case, but we pursue the methods far enough to exhibit the specific calculations needed in order to determine key features of the bifurcation geometry in any given case.

2 The bifurcation map for planar systems

Here we set out the details of the formalism as described by Chicone [7, 8, 9] for applying the method described above to a planar system with one perturbation parameter. We consider the general system

$$\dot{x} = f(x) + \varepsilon g(x, t; \varepsilon) \quad x \in \mathbf{R}^2, \quad \varepsilon \in \mathbf{R} \quad (\mathcal{S}_\varepsilon)$$

in a neighbourhood U of a periodic orbit γ of period $T > 0$ for the system \mathcal{S}_0 (that is, $\varepsilon = 0$), where the maps f and g are assumed to be C^∞ and there are no zeros of f in U . Temporarily disregarding g , we note that at each point $\xi \in U$ we have a basis for (the tangent space to) \mathbf{R}^2

$$\mathcal{B}(\xi) = \{f(\xi), f^\perp(\xi)\}$$

where if $u = (v, w) \in \mathbf{R}^2$ then u^\perp denotes the vector $(-w, v)$. Let $V \subset U$ be the set of zeros of the displacement map P_0 in U , that is the set of T -periodic

orbits in U . For $\xi \in V$ let $\gamma(\xi)$ denote the (T -periodic) orbit of ξ for the unperturbed system \mathcal{S}_0 .

First we suppose that the perturbing vector field g also has period T in t . Then we have Diliberto's result [14] (with minor correction: see [7, 8, 9]):

Theorem 2.1 *The bifurcation map $P' : V \rightarrow \mathbf{R}^2$ has the form*

$$P'(\xi) = (\mathcal{N}(\xi), \mathcal{M}(\xi)) \quad (2.1)$$

with respect to the basis $\mathcal{B}(\xi)$ of \mathbf{R}^2 , where $\mathcal{N}, \mathcal{M} : V \rightarrow \mathbf{R}$ are given by

$$\mathcal{N}(\xi) = \int_0^T \|f\|^{-2} \left\{ f \cdot g - \frac{\alpha(t)}{\beta(t)} f^\perp \cdot g \right\} dt \quad (2.2)$$

$$\mathcal{M}(\xi) = \int_0^T \|f\|^{-2} \left\{ \frac{1}{\beta(t)} f^\perp \cdot g \right\} dt, \quad (2.3)$$

with f, g evaluated at $\xi_t = \phi_t(\xi)$ with $\{\phi_t\}$ the flow for the unperturbed system \mathcal{S}_0 : thus the integrals take place along $\gamma(\xi)$. Here the functions $\alpha(t)$ and $\ln \beta(t)$ correspond to the first-order variation in (respectively) time and displacement transverse to the orbit $\gamma(\xi)$ for orbits of \mathcal{S}_0 close to $\gamma(\xi)$. \square

To be more precise, $\alpha(t)$ and $\beta(t)$ are terms from the fundamental matrix solution $\Psi_\xi(t)$ of the variational equation $\dot{w} = Df(\xi_t)w$ with respect to the bases $\mathcal{B}(\xi)$ and $\mathcal{B}(\xi_t)$ for \mathbf{R}^2 at ξ and ξ_t respectively: we have

$$\Psi_\xi(t) = \begin{pmatrix} 1 & \|f\|^2 \alpha(t) \\ 0 & \beta(t) \end{pmatrix}$$

where explicit formulae for $\alpha(t)$ and $\beta(t)$ can be found in [14] and [7, Theorem 4.1] as well as [8, 9]. However, in the example that we study in this paper the system \mathcal{S}_0 is just simple harmonic motion for which $\alpha(t) = 0$ and $\beta(t) = 1$ for all t , and so the expressions (2.2),(2.3) become

$$\mathcal{N}(\xi) = \int_0^T \|f\|^{-2} f \cdot g dt \quad (2.4)$$

$$\mathcal{M}(\xi) = \int_0^T \|f\|^{-2} f^\perp \cdot g dt. \quad (2.5)$$

In cases when $\alpha \neq 0$ or $\beta \neq 1$ then $\gamma(\xi)$ is called *normally nondegenerate* (see [8, 9]), and in this case $\gamma(\xi)$ is isolated among T -periodic orbits. Finding zeros of P' at points of $\gamma(\xi)$ then reduces (via Liapunov-Schmidt reduction) to studying the zeros of a single function $C : \gamma(\xi) \rightarrow \mathbf{R}$ called the *bifurcation function*. In our applications, however, we do not have normal nondegeneracy and so cannot make this simplification.

2.0.3 The effect of detuning

Suppose now, in contrast to the above, that the t -period T' of $g(x, t; \varepsilon)$ is not exactly T when $\varepsilon \neq 0$. More precisely, suppose that

$$T' = T + k\varepsilon + O(\varepsilon^2)$$

for a nonzero constant $k \in \mathbf{R}$. We call k the *detuning* parameter. It is easy to verify (see [8, end of Section 4]) the following simple but crucial fact:

Proposition 2.2 *The effect of detuning on the map P' is to replace the component \mathcal{N} by $\mathcal{N} + k$. \square*

As might be expected, and as we shall see below, increasing the detuning crucially affects the bifurcation behaviour of \mathcal{S}_ε .

2.0.4 Multiparameter planar systems

For a system \mathcal{S}_ε with multiple parameters $\varepsilon = (\varepsilon_1, \dots, \varepsilon_d) \in \mathbf{R}^d$, where the perturbation term is $\varepsilon \cdot g(x, t; \varepsilon)$ with g taking values in \mathbf{R}^d and the dot denoting scalar product, we apply the above formalism in the case of each scalar parameter ε_i to obtain integrals $\mathcal{N}_i, \mathcal{M}_i$ as in (2.2), (2.3) and construct a matrix-valued bifurcation map $\mathcal{P} : V \rightarrow \mathcal{L}(d, 2)$ as in Section 1.1.2. The van der Pol system (1.1) is of this type with $d = 2$ and $\varepsilon = (\delta, \varepsilon)$.

3 Single van der Pol system

At this point we become more specific and apply the general method described in Section 2 to the single forced van der Pol system (1.1). We have $T = \frac{2\pi}{\omega_0}$ and allow ω to vary with ε so that

$$T' := \frac{2\pi}{\omega} = \frac{2\pi}{\omega_0} + k\varepsilon + O(\varepsilon^2), \quad (3.1)$$

where k is the detuning parameter with a different status from the perturbation parameters δ, ε . For given k we seek those harmonic orbits (T -periodic orbits of (1.1) with $(\delta, \varepsilon) = (0, 0)$) that persist as near-harmonic (T' -periodic) orbits under perturbation with $\varepsilon = (\delta, \varepsilon) \neq (0, 0)$.

3.1 The bifurcation matrix

Evaluation of the integrals that appear in \mathcal{N} and \mathcal{M} in (2.4) and (2.5) is in this case very straightforward, since $\phi_t(\xi) = R_{-t}\xi$ where $\xi = (x, y)^\top$ and R_t

is the 2×2 rotation matrix

$$R_t = \begin{pmatrix} \cos \omega_0 t & -\sin \omega_0 t \\ \sin \omega_0 t & \cos \omega_0 t \end{pmatrix}.$$

Here † denotes transpose; since we are now working with matrices it is necessary to take more care in distinguishing row and column vectors. Taking polar coordinates $(x, y) = (r \cos \theta, r \sin \theta)$ for $r \neq 0$ we find using (2.4), (2.5) (with $T = 2\pi/\omega_0$) that the bifurcation matrix whose columns represent the bifurcation maps for the parameters δ, ε respectively is

$$\mathcal{P}(r, \theta) = \frac{\pi}{\omega_0^2} \begin{pmatrix} 0 & k\pi^{-1}\omega_0^2 - r^{-1} \cos \theta \\ (1 - \frac{1}{4}r^2) & r^{-1} \sin \theta \end{pmatrix}. \quad (3.2)$$

The following results about the kernel $\ker \mathcal{P}(r, \theta)$ are now easy to check:

Proposition 3.1

1. If $\pi \cos \theta - kr\omega_0^2 \neq 0$ and $r \neq 2$ then $\mathcal{P}(r, \theta)$ has zero kernel.
2. If $\pi \cos \theta - kr\omega_0^2 \neq 0$ and $r = 2$ then $\ker \mathcal{P}(r, \theta)$ is spanned by the vector $(1, 0)^\dagger$.
3. If $\pi \cos \theta - kr\omega_0^2 = 0$ and $r \neq 2$ then

$$\ker \mathcal{P}(r, \theta) = \text{span}\{(4 \sin \theta, r(r^2 - 4))^\dagger\}.$$

□

It is the third case that is of most interest to us, since there $\ker \mathcal{P}(r, \theta)$ has dimension 1 and varies with (r, θ) . Thus the two circles C and E given by

$$C : r = 2 \quad (3.3)$$

$$E : r = a \cos \theta, \quad a = \pi(k\omega_0^2)^{-1} \quad (3.4)$$

play a key role in the analysis that follows. Note that E is the circle with diameter $[0, a]$ on the x -axis (we allow $r < 0$, corresponding to replacing θ by $\theta \pm \pi$). As the detuning coefficient k increases the circle E shrinks towards the origin.

The remaining cases not covered by Proposition 3.1 are where $\xi \in E \cap C$, and there the expressions for $\ker \mathcal{P}(r, \theta)$ in cases 2 and 3 coincide *except* where $\sin \theta = 0$. This occurs only at the origin (already excluded since $r \neq 0$) and the point $(2, 0)$ when $a = 2$: at these points $\mathcal{P}(r, \theta)$ is the zero matrix.

3.2 The kernel map

Let \tilde{C}, \tilde{E} denote the circles C, E respectively with (if $a = 2$) the point $(2, 0)$ deleted from C and E and with the origin in any case deleted from E . From Proposition 3.1 we know that $\dim \ker \mathcal{P}(\xi) = 1$ when $\xi \in \tilde{C} \cup \tilde{E}$, and so to each $\xi \in \tilde{C} \cup \tilde{E}$ we can associate the corresponding $\ker \mathcal{P}(\xi)$ as an element of the projective line $\mathbf{R}P^1$ (the set of lines through the origin in \mathbf{R}^2).

Definition 3.2 *The kernel map*

$$\kappa : \tilde{C} \cup \tilde{E} \rightarrow \mathbf{R}P^1$$

is given by

$$\kappa : \xi \mapsto \ker \mathcal{P}(\xi).$$

It is straightforward to verify that κ is a smooth map.

For all $\xi \in \tilde{C}$ we have that $\kappa(\xi)$ is the δ -axis, corresponding to perturbations with zero forcing term. The associated bifurcation map $P'_\delta : \mathbf{R}^2 \rightarrow \mathbf{R}^2$ is identically zero, from which *a priori* we can deduce nothing about the zero set of the displacement map P_δ itself: in particular, it may be empty. However, when $\varepsilon = 0$ the system (1.1) is the standard autonomous van der Pol system (see [25] for example) which is well known to have a unique periodic orbit that tends to the circle C and whose period tends to $2\pi/\omega_0$ as $\delta \rightarrow 0$.

We therefore turn now to the case of $\xi \in \tilde{E}$, where it is the interactions of δ and ε with nonzero detuning k that are important. Here the geometry of the kernel map κ plays a key role. Points $\xi \in E$ can be parametrised as $\xi = \xi(\theta)$ where

$$\xi(\theta) = (r \cos \theta, r \sin \theta)^\dagger = \frac{a}{2}(1 + \cos 2\theta, \sin 2\theta)^\dagger \quad (3.5)$$

for $0 \leq \theta < \pi$, although we shall find it useful to take a ‘double’ parametrization with $0 \leq \theta < 2\pi$. From Proposition 3.1 the geometry of $\kappa : \tilde{E} \rightarrow \mathbf{R}P^1$ is conveniently represented by means of the map $\psi : [0, 2\pi) \rightarrow \mathbf{R}^2$ given by

$$\psi : \theta \mapsto (4 \sin \theta, a \cos \theta (a^2 \cos^2 \theta - 4))^\dagger \quad (3.6)$$

so that $[\psi(\theta)] = \kappa(\xi)$ for $\xi \in \tilde{E}$ given by (3.5), and we write $[\varepsilon]$ to denote the element of $\mathbf{R}P^1$ containing $\varepsilon = (\delta, \varepsilon) \neq (0, 0)$. The image of ψ in \mathbf{R}^2 will be the main tool in our bifurcation analysis.

Definition 3.3 *The bifurcation curve B in \mathbf{R}^2 is the image of the map $\psi : [0, 2\pi) \rightarrow \mathbf{R}^2$.*

It is important to make clear that B itself is not part of any bifurcation diagram for this problem; rather it is the geometry of B that determines the bifurcation diagram as we explain in the remainder of this section.

3.3 Geometry of the bifurcation curve B

As $\xi(\theta)$ traverses E the point $\psi(\theta)$ provides a smooth parametrization of B . Replacing θ by $2\pi - \theta$ reflects B in the ε -axis, while replacing θ by $\theta + \pi \bmod 2\pi$ reflects B in the origin. Thus B exhibits 4-fold symmetry, being setwise invariant under the action of the Klein 4-group generated by these reflections or, equivalently, by reflections in both coordinate axes.

It is of course only the polar angle (mod π) of $\psi(\theta) \in \tilde{B}$ that is significant for describing κ , while the radial distance $|\psi(\theta)|$ is not relevant. This representation of κ nevertheless allows us to take account in a continuous way of the degeneracy at $(x, y) = (2, 0)$ when $a = 2$. The subset $\tilde{B} \subset B$ that corresponds to \tilde{E} consists of B with the points $(\pm 4, 0)$ excluded, and if $a = 2$ the origin excluded also.

3.4 Bifurcation analysis

The first observation is that since $\det \mathcal{P}(r, \theta) \rightarrow \infty$ as $r \rightarrow \infty$ it follows that $\mathcal{P}(\xi)s$ is uniformly bounded away from $0 \in \mathbf{R}^2$ for $s \in S^1$ and ξ outside any neighbourhood of $C \cup E$, and so from (1.5) we deduce that bifurcating near-harmonic orbits must lie close to $C \cup E$. We state this more precisely.

Corollary 3.4 *Given any neighbourhood W of $C \cup E$ in \mathbf{R}^2 and fixed detuning $k \neq 0$ as in (3.1), then for sufficiently small $(\delta, \varepsilon) \neq (0, 0)$ every $\frac{2\pi}{\omega}$ -periodic orbit for the system (1.1) lies in W . \square*

For $\xi \in \tilde{E}$ and $(\delta, \varepsilon) \in \mathbf{R}^2$ we have $(\delta, \varepsilon) \in \ker \mathcal{P}(\xi)$ precisely when the line $[(\delta, \varepsilon)]$ intersects \tilde{B} at $\psi(\theta)$ where $\xi = \xi(\theta)$. We next show that provided this intersection is in general position (transverse) we can deduce the existence of zeros of $P_{(\delta, \varepsilon)}$ close to ξ .

As in Section 1.1.2 we write $(\delta, \varepsilon) = \rho s$ where $s \in S^1$ and $\rho > 0$.

Theorem 3.5 *Suppose $(0, 0) \neq (\delta_0, \varepsilon_0) = \rho_0 s_0 \in \mathbf{R}^2$ and the line $[(\delta_0, \varepsilon_0)]$ intersects \tilde{B} transversely at the point $\psi(\theta_0)$ where $\theta_0 \in [0, 2\pi)$. Let $\xi_0 = \xi(\theta_0) \in \tilde{E}$ and suppose $\xi_0 \notin C$. Let γ_0 denote the harmonic orbit of ξ_0 in \mathbf{R}^2 .*

Then for sufficiently small $\rho > 0$ and s sufficiently close to s_0 the system (1.1) has a $\frac{2\pi}{\omega}$ -periodic orbit close to γ_0 , tending uniformly to γ_0 in all derivatives as $\rho \rightarrow 0$.

Proof. Consider the smooth map

$$G : \mathbf{R}^2 \times S^1 \times \mathbf{R} \rightarrow \mathbf{R}^2$$

given by

$$G(\xi, s, \rho) = P_{\rho s}(\xi) = \rho \mathcal{P}(\xi)s + O(\rho^2)$$

as in (1.5) with $\mathcal{P}(\xi)$ given by (3.2). A solution (ξ, s, ρ) to $G(\xi, s, \rho) = 0$ with $\rho > 0$ corresponds to a T' -periodic orbit of (1.1) through $\xi \in \mathbf{R}^2$ with parameter values $(\delta, \varepsilon) = \rho s$. Since $G(\xi, s, 0)$ vanishes identically we can write

$$G(\xi, s, \rho) = \rho H(\xi, s, \rho)$$

for a smooth map $H : \mathbf{R}^2 \times S^1 \times \mathbf{R} \rightarrow \mathbf{R}^2$ that has the form

$$H(\xi, s, \rho) = \mathcal{P}(\xi)s + O(\rho).$$

To obtain solutions to $H(\xi, s, \rho) = 0$ for small ρ we shall invoke the implicit function theorem.

For $\xi \in \mathbf{R}^2$ and $\varepsilon \in \mathbf{R}^2$ let $\Psi(\xi, \varepsilon) = \mathcal{P}(\xi)\varepsilon$. Thus $\varepsilon \in \ker \mathcal{P}(\xi)$ if and only if $\Psi(\xi, \varepsilon) = 0 \in \mathbf{R}^2$, and for $s \in S^1 \subset \mathbf{R}^2$ we have $\Psi(\xi, s) = H(\xi, s, 0)$.

Let $L = L(\xi, \varepsilon)$ denote the partial derivative of Ψ with respect to ξ at (ξ, ε) .

Lemma 3.6 *Let $\varepsilon \in \ker \mathcal{P}(\xi)$ with $\xi = \xi(\theta) \in \tilde{E}$. The linear map $L : \mathbf{R}^2 \rightarrow \mathbf{R}^2$ is invertible if and only if the line $[\varepsilon]$ intersects \tilde{B} transversely at $\psi(\theta)$. This is equivalent to the condition*

$$\mathbf{a}'(\theta) \cdot \varepsilon \neq 0 \tag{3.7}$$

where $\mathbf{a}(\theta)$ denotes the bottom row of $\mathcal{P}(\xi(\theta))$ for, the prime denotes $d/d\theta$ and the dot denotes scalar product.

Proof. For $\xi \in \mathbf{R}^2$ use polar coordinates $\xi = \xi(r, \theta)$ and write

$$\mathcal{P}(r, \theta) \varepsilon = \begin{pmatrix} v \\ w \end{pmatrix}.$$

Substituting $r = r(\theta) = a \cos(\theta)$ for $\xi \in E$ we have $\xi'(\theta) = (r'(\theta), 1)^\top$ and so

$$L \begin{pmatrix} r'(\theta) \\ 1 \end{pmatrix} = \begin{pmatrix} v'(\theta) \\ w'(\theta) \end{pmatrix} = \begin{pmatrix} 0 \\ w'(\theta) \end{pmatrix} \tag{3.8}$$

since E is defined by $v = 0$. Elementary linear algebra then shows that

$$\det L = \frac{\partial v}{\partial r} w'(\theta) \tag{3.9}$$

so, since $\frac{\partial v}{\partial r} = \cos \theta \neq 0$ for $\xi \in \tilde{E}$, the invertibility of L is equivalent to

$$w'(\theta) = \mathbf{a}'(\theta) \cdot \boldsymbol{\varepsilon} \neq 0$$

as claimed. To see that this characterises transversality of $[\boldsymbol{\varepsilon}]$ to B observe that differentiation of the identity $\mathcal{P}(\xi(\theta))\psi(\theta) = 0$ with respect to θ gives

$$L\xi'(\theta)\psi(\theta) + \mathcal{P}(\xi)\psi'(\theta) = 0. \quad (3.10)$$

The transversality condition is that $\psi'(\theta)$ is *not* a scalar multiple of $\psi(\theta)$, equivalent to $\mathcal{P}(\xi)\psi'(\theta) \neq 0$ and thus by (3.10) to

$$L\xi'(\theta)\psi(\theta) \neq 0$$

which is the condition (3.7) since $\boldsymbol{\varepsilon}$ is a nonzero scalar multiple of $\psi(\theta)$. \square

The proof of Theorem 3.5 now follows, since the IFT implies that if $s_0 \in \ker \mathcal{P}(\xi_0)$ then for s sufficiently close to s_0 and all sufficiently small ρ there is a smooth solution $\xi = \xi(s, \rho)$ to $H(\xi, s, \rho) = 0$ with $\xi(s_0, 0) = \xi_0$. We need consider only $\rho > 0$. The uniform convergence of the corresponding periodic orbit to γ_0 follows from standard smoothness properties of solutions of differential equations. \square

Theorem 3.5 shows that if a ray R from the origin in \mathbf{R}^2 intersects the curve \tilde{B} transversely at one or more points, then each of these points corresponds to a point on the circle E from which a near-harmonic periodic orbit of (1.1) emanates as the parameter point (δ, ε) moves away from the origin along R . However, as the direction of R varies the number of (transverse) intersections of the ray R with B may also vary: typically it will change by 2 each time the ray passes through a nondegenerate (quadratic) tangency with the curve. This is the basis for the following local bifurcation result as first described by Hale and Taboas [20].

Proposition 3.7 *Suppose the ray R_1 has a nondegenerate tangency with the curve B at the point $\psi(\theta_1)$. Then there is a smooth arc Γ_1 from the origin in \mathbf{R}^2 , tangent to R_1 at the origin, such that pairs of fixed points of $F_{(\delta, \varepsilon)}$ close to $\xi(\theta_1) \in \tilde{E}$ (that is, pairs of $\frac{2\pi}{\omega}$ -periodic orbits of (1.1)) are created by a saddle-node bifurcation as (δ, ε) crosses Γ_1 sufficiently close to the origin.*

Proof. The statement clearly holds for solutions to $H(\xi, s, 0) = 0$, in the notation of Theorem 3.5, with $\Gamma_1 = R_1$. The fact that this behaviour persists for $H(\xi, s, \rho) = 0$ for small $\rho > 0$ is a consequence of the local persistence (stability) of nondegenerate tangency. For details of this argument see [20], [12] or [11]. \square

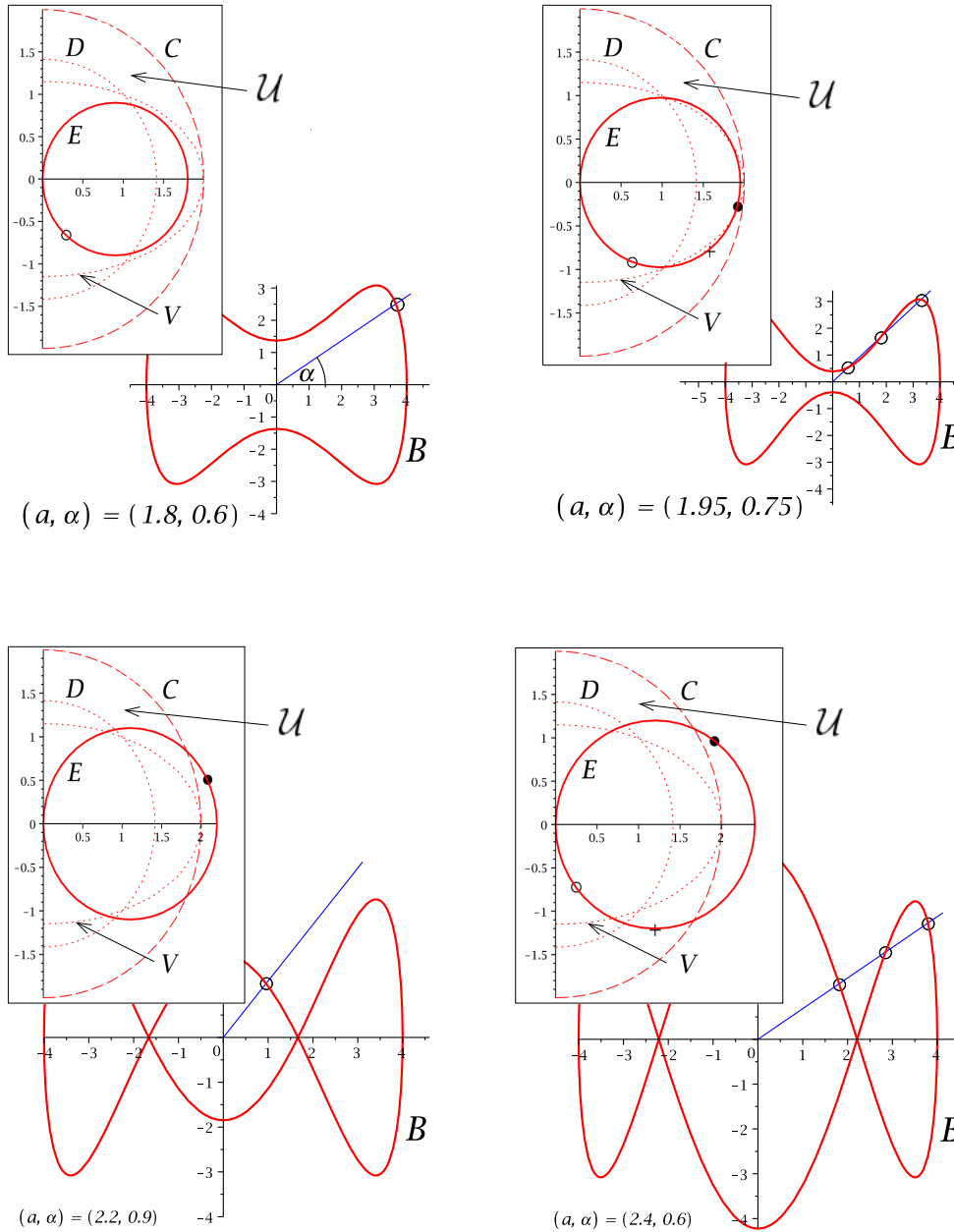


Figure 3.1: The bifurcation curve B in the (δ, ε) -plane for various choices of the (inverse) detuning parameter a , showing intersections of B with a ray from the origin with polar angle α , and (inset) the corresponding points on the circle E in the (x, y) -plane: these are fixed points of the time- T' map $F = F_{(\delta, \varepsilon)}$. The stability of the associated near-harmonic orbits depends on the positions of the fixed points relative to the circles C, D and ellipse V (see Section 3.5). In particular, solid circles • denote stable orbits, while symbols +, ○ denote those with one or both eigenvalues (respectively) of the derivative of F lying outside the unit circle.

In Figure 3.1 we show plots of the curve B for various choices of the parameter a (proportional to k^{-1} as in (3.4)), here chosen with $a > 0$, together with certain choices of rays through the origin that intersect B transversely. We also show the points on E associated to these intersections, that is the corresponding points $\xi \in \mathbf{R}^2$ from which near-harmonic periodic orbits of the perturbed system will bifurcate as in Theorem 3.5.

We now describe this behaviour more precisely in the following theorem which is the main result of this paper for the single van der Pol system (1.1).

Denote by $R(\alpha)$ the ray R that makes an angle α (its polar angle) with the positive δ -axis. As the figures suggest, rays $R(\alpha)$ are typically transverse to or have nondegenerate tangency with B , although there is precisely one value $a = a_2$ at which rays $R(\alpha)$ with polar angles $\pm\alpha_2$ and $\pi \pm\alpha_2$ have cubic tangency with B .

In the ξ -plane let E^+, E^- denote the upper ($y > 0$) and lower ($y < 0$) semicircles of E respectively. In the (δ, ε) -plane, number the quadrants anticlockwise in the usual way, starting with the first quadrant where δ, ε are both positive.

Theorem 3.8 *First suppose $a > 0$. There are three ranges of a in which behaviour differs.*

$$(1) \quad 0 < a \leq a_2 = \frac{4\sqrt{2}}{3} \sim 1.89 \quad (\text{that is } k \geq k_2 = \frac{3\pi}{4\sqrt{2}}\omega_0^2).$$

For $a < a_2$ there is for each α precisely one intersection of $R(\alpha)$ with B . It is transverse, and for $\alpha \neq 0, \pi$ (that is $\varepsilon \neq 0$) corresponding to a T' -periodic point ξ lying in E^- or E^+ according as α lies in an odd or even quadrant, with ξ tending to the origin or $(a, 0)$ as α tends to an even or odd multiple of $\frac{\pi}{2}$ respectively. For $a = a_2$ there is a cubic tangency of $R(\alpha_2)$ with B , where $\tan(\alpha_2) = \pm\frac{4\sqrt{2}}{3\sqrt{3}} \sim \pm 1.09$.

$$(2) \quad a_2 < a < 2 \quad (\text{that is } \frac{\pi}{2\omega_0^2} = k_1 < k < k_2).$$

In each quadrant there are precisely two values $\alpha_1(a), \tilde{\alpha}_1(a)$ of α for which $R(\alpha)$ is tangent to B , the tangencies being nondegenerate. For α in the sector $S(a)$ between α_1 and $\tilde{\alpha}_1$ the ray $R(\alpha)$ has three (transverse) intersections with B , while for α outside the closure of $S(a)$ there is only one. All the corresponding T' -periodic points $\xi \in E$ lie in E^- or E^+ according as α lies in an odd or even quadrant. These periodic points ξ are created or annihilated in pairs at saddle-node (quadratic) bifurcations as α passes through α_1 and $\tilde{\alpha}_1$. As α tends to an even or odd multiple of $\frac{\pi}{2}$ (that is $\varepsilon \rightarrow 0$ or $\delta \rightarrow 0$) the (single) corresponding ξ tends to the origin or to $(a, 0)$ respectively.

(3) $a > 2$ (that is $0 < k < k_1$).

For $\alpha \neq 0, \pi$ each ray $R(\alpha)$ has transverse intersection with B at a point $\psi(\xi_0)$ with the corresponding T' -periodic point ξ_0 lying in E^- or E^+ according as $R(\alpha)$ lies in an even or odd quadrant. The point ξ_0 varies smoothly with α and a , and ξ_0 tends to $(a, 0)$ as $\alpha \rightarrow \pm \frac{\pi}{2}$.

Moreover, there is also a unique value $\alpha_1(a)$ for which $R(\alpha_1)$ has a non-degenerate quadratic tangency with B . For $R(\alpha)$ lying between $R(\alpha_1)$ and the x -axis the ray $R(\alpha)$ has two further transverse intersections with B . These correspond to T' -periodic points ξ_1, ξ_2 in the opposite semicircle of E from ξ_0 , created at a saddle-node bifurcation as α passes through α_1 . One of ξ_1 or ξ_2 tends to the origin as $\alpha \rightarrow 0$ or $\alpha \rightarrow \pi$.

Note: when $a = 2$ the curve B passes through the origin and the analysis there in terms of $\ker \mathcal{P}(\xi)$ breaks down.

Finally, when $a < 0$ the descriptions are analogous, after reflecting the circle E through the origin while reflecting the curve B in the δ -axis.

Proof. The condition that $\psi(\theta)$ and $\psi'(\theta)$ be linearly dependent, corresponding to a tangency of $R(\alpha)$ with B at $\psi(\theta)$, is easily verified from (3.5) and (3.6) to be

$$2a^2u^2 - 3a^2u + 4 = 0 \tag{3.11}$$

where $u = \cos^2 \theta$. This is easily checked to be the same as the condition that $\mathbf{a}'(\theta) \cdot (\delta, \varepsilon) = 0$: compare (3.7). For $0 < a < a_2$ this equation has no real solutions u . As a increases through a_2 a pair of solutions is created at $u = \frac{3}{4}$ (corresponding to $\theta = \pi \pm \frac{\pi}{6}$): one of these solutions increases through $u = 1$ (that is $\theta = \pi$) as a increases through 2, and the other solution remains in the interval $(0, \frac{3}{4})$ for all a . Reinterpreting these statements in terms of θ gives the results as described. \square

In the (a, α) -parameter space this behaviour is organised by a cusp bifurcation at (a_2, α_2) as shown in Figure 3.2.

Using the structural stability of cusp (codimension 2) bifurcations and Proposition 3.7 we can describe the bifurcation behaviour for (1.1) for (δ, ε) close to the origin as $|a|$ passes through a_2 .

Corollary 3.9 *For each $|a| > 2$ there is in each quadrant of the (δ, ε) parameter plane a unique smooth arc $\Gamma_0(a)$ from the origin such that a saddle-node bifurcation of periodic orbits with angular frequency ω close to ω_0 occurs as (δ, ε) crosses $\Gamma_0(a)$ sufficiently close to the origin. For $a_2 < |a| < 2$ there are two such arcs $\Gamma_0(a), \tilde{\Gamma}_0(a)$ which approach each other and mutually annihilate as $|a|$ decreases through a_2 . \square*

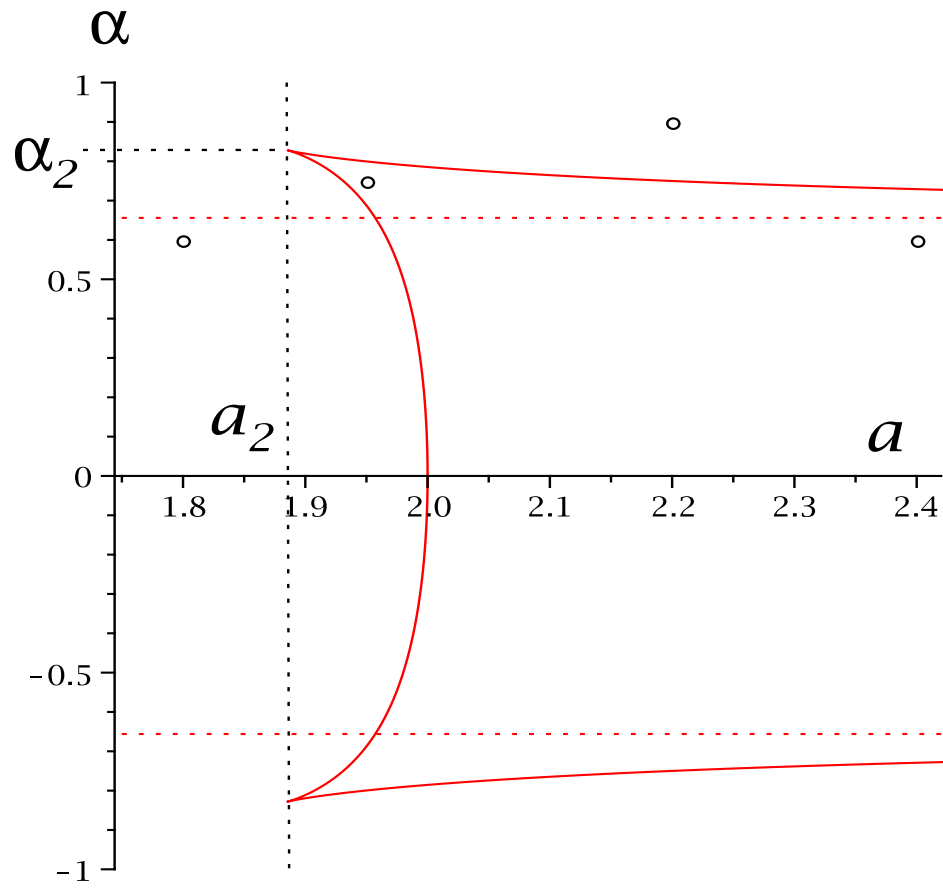


Figure 3.2: Bifurcation diagram in the limit as $\rho \rightarrow 0$ for the system (1.1) with detuning k as in (3.1). Here $a = \pi(k\omega_0^2)^{-1}$ and $(\delta, \varepsilon) = \rho(\cos \alpha, \sin \alpha)$. The curve corresponds to saddle-node bifurcations of $\frac{2\pi}{\omega}$ -periodic orbits, with cusp bifurcation points at $(a_2, \pm\alpha_2)$. Small circles indicate the parameter values corresponding to the diagrams in Figure 3.1.

3.5 Stability

The preceding bifurcation analysis considered only the existence of near-harmonic periodic orbits and not their stability. A periodic orbit of \mathcal{S}_ε corresponding to a fixed point ξ of F_ε is linearly asymptotically stable precisely when the eigenvalues of $DF_\varepsilon(\xi)$ lie inside the unit circle. If $\varepsilon = \rho s$ for $s \in S^1, \rho > 0$ as before we have

$$DF_\varepsilon(\xi) = I + \rho L + O(\rho^2)$$

with I the identity and $L \in \mathcal{L}(2, 2)$ as in the proof of Lemma 3.6. The eigenvalues of $DF_\varepsilon(\xi)$ thus have the form $1 + \rho\lambda + O(\rho^2)$ for λ an eigenvalue of L . It follows that, for ρ sufficiently small, an eigenvalue of $DF_\varepsilon(\xi)$ lies inside the unit circle if and only if the corresponding eigenvalue of L has negative real part, which we can determine from the trace and determinant of L .

To evaluate the trace and determinant we must use the same coordinates in domain and range, while we recall that the matrix $\mathcal{P}(\xi)$ is defined using the basis $\mathcal{B}(\xi)$ in the range. Therefore we need first to rotate and re-scale $\mathcal{B}(\xi)$ back to the standard basis, that is to multiply $\mathcal{P}(\xi)$ on the left by the matrix $\omega_0 \begin{pmatrix} y & x \\ -x & y \end{pmatrix}$, after which we easily find that for arbitrary $s = (d, e) \in S^1$ and $\xi \in \mathbf{R}^2$

$$\text{trace } L = \frac{\pi}{\omega_0} d(2 - r^2).$$

We also find

$$\det L = \frac{\pi^2}{16\omega_0^2} (d^2(4 - r^2)(4 - 3r^2) + 16e^2 a^{-2})$$

which for $\xi = (x, y) \in E$ and $s \in \ker \mathcal{P}(\xi)$ becomes

$$\det L = \frac{\pi^2}{\omega_0^2} (r^2 - 4)(x^2 + 3y^2 - 4)$$

after using (3.5), (3.6). From this we see that the real parts of both eigenvalues of L are negative if and only if $\xi = (x, y) \notin \mathcal{U}$ and d has the same sign as $r^2 - 2$. Therefore we arrive at the following characterisation of stability.

Proposition 3.10 *Let $\varepsilon = (\delta, \varepsilon) = \rho s \in \mathbf{R}^2$ and assume that the line $[\varepsilon]$ intersects the bifurcation curve B transversely at a point $\psi(\theta_0) \in \tilde{B}$. Then for $\rho > 0$ sufficiently small, the near-harmonic periodic orbit for \mathcal{S}_ε bifurcating from the harmonic orbit γ_0 of $\xi_0 = \xi(\theta_0)$ is linearly asymptotically stable if and only if ξ_0 lies outside the region \mathcal{U} and outside or inside the circle $D = \{\xi : |\xi| = \sqrt{2}\}$ according as $\delta > 0$ or $\delta < 0$. \square*

For example, in Figure 3.1 for $(a, \alpha) = (1.8, 0.6)$ there are no linearly asymptotically stable bifurcating periodic orbits: here $\delta > 0$ and the only bifurcating periodic point $\xi \in E$ lies outside the region \mathcal{U} but inside the circle D . With α replaced by $\alpha + \pi$, however, the location of ξ is unchanged but the bifurcating periodic orbit becomes stable. Likewise for the other three cases shown: it is only the periodic point ξ not in \mathcal{U} and lying outside D that is stable. The existence and stabilities of these periodic orbits may be easily verified using the package *DEtools* in Maple, for example.

Thus we see that the ‘double’ parametrization of the circle E , while technically redundant as far as existence of T' -periodic orbits is concerned, nevertheless plays a role in their stability analysis.

This concludes the bifurcation analysis for near-harmonic periodic orbits for a single forced van der Pol system with detuning, based on the study of the kernel of the bifurcation matrix and the geometry of its movement as parameters are varied. We now turn to apply this technique to the more complicated case of a coupled pair of systems of the same van der Pol type.

4 A coupled pair of forced van der Pol equations

In this section we study a system of equations of the form

$$\begin{aligned} \dot{u}_1 &= v_1 \\ \dot{v}_1 &= -u_1 - c_1 u_2 + h_1 \\ \dot{u}_2 &= v_2 \\ \dot{v}_2 &= -c_2 u_1 - u_2 + h_2 \end{aligned} \tag{4.1}$$

where the coupling terms c_1, c_2 are positive constants with $c_1 c_2 < 1$ to ensure that the unperturbed linear system (with $h_1 = h_2 = 0$) has purely imaginary eigenvalues. The terms h_1, h_2 are as yet unspecified but considered to be smooth functions of t with small amplitude. We first set up the machinery to calculate the 4×4 bifurcation matrix for the general system (4.1) and then specialise to the case of two van der Pol systems.

We do not attempt a full description of the bifurcation of near-harmonic periodic orbits, but describe the details of the geometric framework in \mathbf{R}^4 analogous to the 2-dimensional characterisations for a single system illustrated in Figure 3.1 and obtain some intermediate results. In the regime that will be of interest to us the kernel of the bifurcation matrix is 2-dimensional while (u_1, v_1, u_2, v_2) lies on a certain torus in \mathbf{R}^4 . This torus is the analog of

the circle E in Section 3, and so the bifurcation of near-harmonic periodic orbits is now described in terms of a 2-parameter family of 2-planes through the origin in 4-space. After stereographic projection this can be interpreted as a *line congruence* in \mathbf{R}^3 .

4.1 Constructing the bifurcation matrix

We begin by applying a linear transformation

$$\begin{pmatrix} u_1 \\ v_1 \\ u_2 \\ v_2 \end{pmatrix} = \begin{pmatrix} 1 & 0 & 1 & 0 \\ 0 & \omega_1 & 0 & \omega_2 \\ d & 0 & -d & 0 \\ 0 & \omega_1 d & 0 & -\omega_2 d \end{pmatrix} \begin{pmatrix} y_1 \\ z_1 \\ y_2 \\ z_2 \end{pmatrix} \quad (4.2)$$

to put the system (4.1) into the slightly more amenable form

$$\dot{y}_1 = \omega_1 z_1 \quad (4.3)$$

$$\dot{z}_1 = -\omega_1 y_1 + \frac{1}{2\omega_1}(h_1 + ch_2) \quad (4.4)$$

$$\dot{y}_2 = \omega_2 z_2 \quad (4.5)$$

$$\dot{z}_2 = -\omega_2 y_2 + \frac{1}{2\omega_2}(h_1 - ch_2). \quad (4.6)$$

Here

$$1 - \omega_2^2 = \sqrt{c_1 c_2} = \omega_1^2 - 1 \quad (4.7)$$

and $c = d^{-1} = \pm \sqrt{\frac{c_1}{c_2}}$, while the terms h_1, h_2 are now understood to be expressed in terms of the new coordinates. We suppose moreover that ω_1, ω_2 are rationally related, so that $n\omega_1 = m\omega_2$ for integers n, m and therefore all orbits of the linear system are periodic.

Now suppose that h_i ($i = 1, 2$) in (4.4),(4.6) depend smoothly on a single parameter $\varepsilon \in \mathbf{R}$ and vanish when $\varepsilon = 0$, so that

$$h_i = \varepsilon g_i + O(\varepsilon^2)$$

for smooth functions g_i and $i = 1, 2$. Applying the general theory outlined above in Section 1.1.1 and again following Chicone [8, 9, 10] we have associated to ε a bifurcation map

$$P' = (\mathcal{N}_1, \mathcal{N}_2, \mathcal{M}_1, \mathcal{M}_2)^\dagger : V \rightarrow \mathbf{R}^4 \quad (4.8)$$

where

$$\mathcal{N}_1 = \int_0^T \frac{-y_1}{2\|f_1\|^2} (g_1 + cg_2) dt \quad (4.9)$$

$$\mathcal{N}_2 = \int_0^T \frac{-y_2}{2\|f_2\|^2} (g_1 - cg_2) dt \quad (4.10)$$

$$\mathcal{M}_1 = \int_0^T \frac{z_1}{2\|f_1\|^2} (g_1 + cg_2) dt \quad (4.11)$$

$$\mathcal{M}_2 = \int_0^T \frac{z_2}{2\|f_2\|^2} (g_1 - cg_2) dt. \quad (4.12)$$

Here $T = 2m\pi/\omega_1 = 2n\pi/\omega_2$, and the integrals are taken along a T -periodic (harmonic) solution curve γ for the unperturbed system ($\varepsilon = 0$). The solution for γ is given explicitly by

$$(y_i(t), z_i(t))^{\mathfrak{t}} = (r_i \cos(\omega_i t + \theta_i), r_i \sin(\omega_i t + \theta_i))^{\mathfrak{t}}, \quad i = 1, 2.$$

4.2 The van der Pol case

We now specialise to the particular choices of h_1, h_2 that correspond to van der Pol systems, namely

$$h_i = \delta_i v_i (1 - u_i^2) + \varepsilon_i \cos(\tilde{\omega}_i t) \quad (4.13)$$

for $i = 1, 2$. Here the forcing angular frequency $\tilde{\omega}_i$ is close to ω_i , so that as in (3.1)

$$\frac{2\pi}{\tilde{\omega}_i} = \frac{2\pi}{\omega_i} + \kappa_i \varepsilon_i + O(\varepsilon_i^2) \quad (4.14)$$

with κ_i the detuning parameter for $i = 1, 2$, and we seek periodic solutions of period $T' = 2m\pi/\tilde{\omega}_1 = 2n\pi/\tilde{\omega}_2$.

To construct the bifurcation matrix as in Section 1.1.2 it is necessary to evaluate the four integrals (4.9)–(4.12) for each of the four cases corresponding to the components of $\varepsilon = (\delta_1, \delta_2, \varepsilon_1, \varepsilon_2)$ in turn. The results are set out below. Additional terms appear if $\omega_1 = \omega_2$ (already excluded by (4.7)) or $3\omega_1 = \omega_2$ (likewise) or $\omega_1 = 3\omega_2$, and so for simplicity we exclude this latter resonant case.

Case 1: parameter δ_1

$$\left. \begin{aligned} g_1 &= v_1(1 - u_1^2) = (\omega_1 z_1 + \omega_2 z_2)(1 - (y_1 + y_2)^2) \\ g_2 &= 0 \end{aligned} \right\}.$$

Here we find $\mathcal{N}_1 = \mathcal{N}_2 = 0$ while

$$\mathcal{M}_i = \frac{T}{16\omega_i}(p + r_i^2) \quad (4.15)$$

for $i = 1, 2$, where $p = 4 - 2(r_1^2 + r_2^2)$.

Case 2: parameter δ_2

$$\left. \begin{aligned} g_1 &= 0 \\ g_2 &= v_2(1 - u_2^2) = d(\omega_1 z_1 - \omega_2 z_2)(1 - d^2(y_1 - y_2)^2) \end{aligned} \right\}.$$

Again $\mathcal{N}_1 = \mathcal{N}_2 = 0$ and now

$$\mathcal{M}_i = \frac{T}{16\omega_i}(q + d^2 r_i^2) \quad (4.16)$$

for $i = 1, 2$, where $q = 4 - 2d^2(r_1^2 + r_2^2)$.

Case 3: parameter ε_1

$$g_1 = \cos \tilde{\omega}_1 t, \quad g_2 = 0.$$

Here using Proposition 2.2 we find

$$\mathcal{N}_1 = -\frac{T}{4\omega_1^2 r_1} \cos \theta_1 + m\kappa_1, \quad \mathcal{M}_1 = \frac{T}{4\omega_1^2 r_1} \sin \theta_1 \quad (4.17)$$

while $\mathcal{N}_2 = \mathcal{M}_2 = 0$.

Case 4: parameter ε_2

$$g_1 = 0, \quad g_2 = \cos \tilde{\omega}_2 t.$$

Here

$$\mathcal{N}_2 = \frac{cT}{4\omega_2^2 r_2} \cos \theta_2 + n\kappa_2, \quad \mathcal{M}_2 = -\frac{cT}{4\omega_2^2 r_2} \sin \theta_2 \quad (4.18)$$

while $\mathcal{N}_1 = \mathcal{M}_1 = 0$.

The above calculations provide the four columns of the 4×4 bifurcation matrix corresponding to the parameters $\delta_1, \delta_2, \varepsilon_1, \varepsilon_2$ in turn. Assembling the matrix we thus obtain

$$\mathcal{P}(\xi) = \frac{T}{16} \begin{pmatrix} 0 & 0 & -a_1 \cos \theta_1 + d_1 & 0 \\ 0 & 0 & 0 & a_2 c \cos \theta_2 + d_2 \\ \omega_1^{-1}(p + r_1^2) & \omega_1^{-1}(q + d^2 r_1^2) & a_1 \sin \theta_1 & 0 \\ \omega_2^{-1}(p + r_2^2) & \omega_2^{-1}(q + d^2 r_2^2) & 0 & -a_2 c \sin \theta_2 \end{pmatrix} \quad (4.19)$$

where

$$\xi = (r_1 \cos \theta_1, r_1 \sin \theta_1, r_2 \cos \theta_2, r_2 \sin \theta_2) \quad (4.20)$$

and where $a_i = 4r_i^{-1}\omega_i^{-2}$, $r_i \neq 0$ and $d_i = \frac{8}{\pi}\omega_i\kappa_i$ for $i = 1, 2$. Note that here a_1, a_2 are analogs of the inverse-detuning parameter a in Section 3, not to be confused with the specific parameter value a_2 in Proposition 3.8.

Following Proposition 1.3 we seek the kernel of the matrix $\mathcal{P}(\xi)$. First, we find

$$\det \mathcal{P}(\xi) = K\Delta(-a_1 \cos \theta_1 + d_1)(a_2c \cos \theta_2 + d_2) \quad (4.21)$$

where $\Delta = (1 - d^2)(r_1^2 - r_2^2)$ and K is a positive constant.

Write

$$p_i = (p + r_i^2) \quad \text{and} \quad q_i = (q + d^2r_i^2) \quad \text{for } i = 1, 2,$$

and let

$$b_1 = -a_1 \cos \theta_1 + d_1 \quad (4.22)$$

$$b_2 = a_2c \cos \theta_2 + d_2. \quad (4.23)$$

The following facts are easily verified:

Proposition 4.1

(1) *If $b_1 = 0$ and $b_2\Delta \neq 0$ then $\mathcal{P}(\xi)$ has rank 3 and $\ker \mathcal{P}(\xi)$ is spanned by the vector*

$$\boldsymbol{\mu}_1(\xi) := (q_2a_1 \sin \theta_1, -p_2a_1 \sin \theta_1, -4\omega_1^{-1}\Delta, 0)^\dagger.$$

(2) *If $b_2 = 0$ and $b_1\Delta \neq 0$ then $\mathcal{P}(\xi)$ has rank 3 and $\ker \mathcal{P}(\xi)$ is spanned by the vector*

$$\boldsymbol{\mu}_2(\xi) := (-cq_1a_2 \sin \theta_2, cp_1a_2 \sin \theta_2, 0, 4\omega_2^{-1}\Delta)^\dagger.$$

(3) *If $b_1b_2 \neq 0$ and $\Delta = 0$ then $\mathcal{P}(\xi)$ has rank 3 and $\ker \mathcal{P}(\xi)$ is spanned by the vector*

$$\boldsymbol{\nu}(\xi) := (q_1, -p_1, 0, 0)^\dagger.$$

(4) *If $b_1 = b_2 = 0$ and $\Delta \neq 0$ then $\mathcal{P}(\xi)$ has rank 2 and $\ker \mathcal{P}(\xi)$ is spanned by the vectors $\{\boldsymbol{\mu}_1(\xi), \boldsymbol{\mu}_2(\xi)\}$.*

□

Denote the subsets of \mathbf{R}^4 on which the conditions (1)–(4) hold by N_1, N_2, N_3, N_4 respectively. In case (1) the vector $\boldsymbol{\mu}_1(\xi)$ is independent of θ_2 and so the kernel map

$$\kappa : N_1 \rightarrow \mathbf{R}P^3 : \xi \rightarrow \ker \mathcal{P}(\xi)$$

is degenerate; likewise for the map $\kappa : N_2 \rightarrow \mathbf{R}P^3$. In case (3) the vector $\boldsymbol{\nu}(\xi)$ depends on neither θ_1 nor θ_2 and so κ has even greater degeneracy. However, in case (4), where $\dim \ker \mathcal{P}(\xi) = 2$, we have a more amenable situation, as we shall next show.

4.3 The first order bifurcation problem

In order to build a framework for describing the configuration of solutions to $P_\varepsilon = 0$ (corresponding to near-harmonic periodic solutions of (4.1)) analogous to the circle E and curve B for the single system (1.1) but now in higher dimensions, we introduce the following terminology:

$$\begin{aligned} M &:= \{(\xi, \varepsilon) \in \mathbf{R}^4 \times \mathbf{R}^4 : P_\varepsilon(\xi) = 0\}, \\ M^L &:= \{(\xi, \varepsilon) \in \mathbf{R}^4 \times \mathbf{R}^4 : \mathcal{P}(\xi)\varepsilon = 0\}. \end{aligned}$$

Thus M is the locus of solutions that we seek (at least for $|\varepsilon|$ small), while M^L is the locus of solutions for the simpler system obtained when terms of order greater than 1 in the parameters are ignored. We call this latter problem the *first order bifurcation problem*, and regard M^L as a close approximation to M for small values of $|\varepsilon|$. We discuss below the extent to which this is justified.

Let

$$pr : \mathbf{R}^4 \times \mathbf{R}^4 \rightarrow \mathbf{R}^4$$

denote projection to the second (that is, the ε) factor. The overall bifurcation behaviour of the displacement map P_ε is determined by the geometry of the projection $pr|M : M \rightarrow \mathbf{R}^4$, since if $\varepsilon \in \mathbf{R}^4$ then $M \cap pr^{-1}(\varepsilon)$ is by definition the set of points (ξ, ε) such that ξ satisfies $P_\varepsilon(\xi) = 0$ for the given ε , and as ε varies the structure of $M \cap pr^{-1}(\varepsilon)$ may change. An analogous statement applies to $pr|M^L$ and the solutions to $\mathcal{P}(\xi)\varepsilon = 0$.

If $(\xi_0, \varepsilon_0) \in M$ is such that ξ_0 is a regular point of P_{ε_0} then, by the IFT, the solution locus M is locally a smooth 4-manifold in a neighbourhood of (ξ_0, ε_0) and such that the projection $pr|M : M \rightarrow \mathbf{R}^4$ is a local diffeomorphism at (ξ_0, ε_0) . Specifically, for all ε sufficiently close to ε_0 there is a unique $\xi = \xi(\varepsilon)$ close to ξ_0 and varying smoothly with ε such that $P_\varepsilon(\xi) = 0$. Consequently bifurcation can occur only where ξ is not a regular point of P_ε , in which

case *either* M fails locally to be a smooth 4-manifold *or* M is a 4-manifold but (ξ, ε) is a singular point of the projection $pr|M : M \rightarrow \mathbf{R}^4$. Analogous statements apply to M^L with the map $\xi \mapsto \mathcal{P}(\xi)\varepsilon$ in place of P_ε . We write

$$\begin{aligned}\Xi &:= \{(\xi, \varepsilon) \in M : \xi \text{ is a singular point of } P_\varepsilon\} \\ \Xi^L &:= \{(\xi, \varepsilon) \in M^L : \xi \text{ is a singular point of } \xi \mapsto \mathcal{P}(\xi)\varepsilon\}.\end{aligned}$$

Definition 4.2 *The bifurcation set Γ or Γ^L for the nonlinear problem or for the first-order problem respectively is the subset $\Gamma = pr(\Xi)$ or $\Gamma^L = pr(\Xi^L)$ of the parameter space \mathbf{R}^4 .*

Our strategy in the bifurcation analysis, which mimics that of Section 3, is to characterise those features of the singularity geometry of the map

$$pr|M^L : M^L \rightarrow \mathbf{R}^4$$

that are robust, i.e. persist under sufficiently small perturbations, and then deduce that those features will also be present in the projection

$$pr|M : M \rightarrow \mathbf{R}^4$$

for ε sufficiently close to the origin in parameter space \mathbf{R}^4 . This will justify our view of M^L as an accurate model for M when parameter values are small. In order to make these ideas precise we shall use results from singularity theory.

The degeneracies in cases (1)–(3) of Proposition 4.1 imply that we cannot expect robustness in the structure of the projection $M^L \rightarrow \mathbf{R}^4$ near points (ξ, ε) where $\xi \in N_1 \cup N_2 \cup N_3$. In the remainder of the paper we therefore deal only with case (4) where $\xi \in N = N_4$.

4.3.1 Structure of the singularities when $\xi \in N$

In the phase space $\mathbf{R}^4 = \mathbf{R}^2 \times \mathbf{R}^2$ the manifold N is the torus given by

$$(d_1, d_2) = (a_1 \cos \theta_1, -a_2 c \cos \theta_2),$$

that is in polar coordinates

$$\xi = (r_1 \cos \theta_1, r_1 \sin \theta_1, r_2 \cos \theta_2, r_2 \sin \theta_2) \quad (4.24)$$

where

$$(r_1, r_2) = (2t_1 \cos \theta_1, -2t_2 \cos \theta_2) \quad (4.25)$$

with $r_1 r_2 \neq 0$, $r_1^2 \neq r_2^2$ and

$$4t_i = \pi \omega_i^{-3} \kappa_i^{-1} \chi_i \quad (4.26)$$

for $\chi_1 = 1$ and $\chi_2 = c$. We allow $r_i < 0$ when $\frac{\pi}{2} < \theta_i < \frac{3\pi}{2} \pmod{2\pi}$. This torus is the analog of the circle $E \subset \mathbf{R}^2$ in the case of the single van der Pol system in Section 3.

From Proposition 4.1 we have an explicit parametrization of the 4-dimensional solution locus

$$N^L := M^L \cap (N \times \mathbf{R}^4),$$

namely

$$\Phi : (\theta_1, \theta_2, x, y) \mapsto (\xi(\theta_1, \theta_2), x\boldsymbol{\mu}_1(\theta_1, \theta_2) + y\boldsymbol{\mu}_2(\theta_1, \theta_2)) \quad (4.27)$$

where $\xi(\theta_1, \theta_2)$ is as in (4.24) with (r_1, r_2) given by (4.25), and with $\boldsymbol{\mu}_1, \boldsymbol{\mu}_2$ expressed in terms of (θ_1, θ_2) also using (4.25). Since for all $\lambda \in \mathbf{R}$ we have

$$\mathcal{P}(\xi)\lambda\boldsymbol{\varepsilon} = \lambda\mathcal{P}(\xi)\boldsymbol{\varepsilon}, \quad (4.28)$$

in order to find the singular set Ξ^L for the projection $N^L \rightarrow \mathbf{R}^4$ it will suffice to restrict $\boldsymbol{\varepsilon} \in \mathbf{R}^4$ to $|\boldsymbol{\varepsilon}| = 1$ and then extend radially in parameter space. For this purpose for any $\rho > 0$ denote

$$\begin{aligned} M_\rho &:= M \cap (\mathbf{R}^4 \times \rho S^3), \\ M_\rho^L &:= M^L \cap (\mathbf{R}^4 \times \rho S^3) \end{aligned}$$

where $S^3 \subset \mathbf{R}^4$ is the unit 3-sphere. We focus attention on M_1^L and in particular on

$$N_1^L := N^L \cap M_1^L.$$

The projection of N^L into parameter space \mathbf{R}^4 can be viewed as a 2-parameter family \mathcal{A} of 2-planes through the origin in \mathbf{R}^4 , these being the 2-dimensional kernels of $\mathcal{P}(\xi)$ with $\xi = \xi(\theta_1, \theta_2) \in N$. The projection of N_1^L into S^3 can likewise be seen as a 2-parameter family $\mathcal{A} \cap S^3$ of great circles, and by (4.28) the family \mathcal{A} has the structure of a cone from the origin to $\mathcal{A} \cap S^3$. However, in order to visualise \mathcal{A} , rather than work in S^3 we instead project $\mathcal{A} \cap S^3$ radially to $\mathcal{A} \cap \Pi$ for a fixed affine 3-space Π not through the origin in \mathbf{R}^4 : then $\mathcal{A} \cap \Pi$ is a 2-parameter family of lines in Π , also called a *line congruence* in Π . This line congruence structure provides an effective way to grasp the local geometry of the bifurcation set Γ^L .

Conveniently, the local geometry of line congruences has been studied and classified using methods of singularity theory by Izumiya *et al.* [22].

In that paper the authors show that the singularities that arise in generic line congruences are the same as those that arise in generic smooth maps $\mathbf{R}^3 \rightarrow \mathbf{R}^3$, namely *folds*, *cusps* and *swallowtail* points. These are also stable singularities: their local structure persists (up to smooth coordinate change in source and target) under sufficiently small smooth perturbations.

In view of these results, together with the fact that radial projection from the origin is a diffeomorphism from a hemisphere of S^3 to Π , we expect $\Xi_1^L := \Xi^L \cap N_1^L$ to consist of fold surfaces, possibly with curves of cusp points and isolated swallowtail points, their configuration determining the bifurcation structure for the first order bifurcation problem $\mathcal{P}(\xi)\boldsymbol{\varepsilon} = 0$ with $|\boldsymbol{\varepsilon}| = 1$. To confirm whether this is the case in the current setting it would be necessary to verify when the genericity assumptions used in [22] hold also in our context of coupled van der Pol systems. We do not attempt this here, but instead provide algebraic and geometric criteria that explicitly characterise fold, cusps and swallowtail points in this context. Moreover, we give numerical illustrations confirming that all these do in fact occur.

4.3.2 The singular set Ξ_1^L

For convenience we choose Π to be the hyperplane given by $\varepsilon_1 = 1$ in \mathbf{R}^4 . (This choice excludes points of Ξ^L lying in the hyperplane $\varepsilon_1 = 0$ of course.) Accordingly we replace $\boldsymbol{\mu}_1, \boldsymbol{\mu}_2$ by scalar multiples of themselves that have first component equal to 1, and then focus on the remaining three components. Explicitly, assuming $\sin \theta_1, \sin \theta_2 \neq 0$ and writing

$$\boldsymbol{\mu}_1 = q_2 a_1 \sin \theta_1 (1, \boldsymbol{\nu}_1), \quad \boldsymbol{\mu}_2 = -c q_1 a_2 \sin \theta_2 (1, \boldsymbol{\nu}_2)$$

with $\boldsymbol{\nu}_1, \boldsymbol{\nu}_2 \in \mathbf{R}^3$, we replace Φ in (4.27) by the reduced map

$$\tilde{\Phi} : (\theta_1, \theta_2, x) \mapsto (\xi(\theta_1, \theta_2), x\boldsymbol{\nu}_1(\theta_1, \theta_2) + (1-x)\boldsymbol{\nu}_2(\theta_1, \theta_2))$$

that parametrises the 3-manifold $N_\Pi^L := M^L \cap (N \times \Pi)$. In order to study the singularities of the projection $N_\Pi^L \rightarrow \Pi$, and so by radial extension the singularity set Ξ^L , we are thus led to study the singularities of the map

$$G : U \times \mathbf{R} \rightarrow \mathbf{R}^3 : (\theta_1, \theta_2, x) \mapsto x\boldsymbol{\nu}_1(\theta_1, \theta_2) + (1-x)\boldsymbol{\nu}_2(\theta_1, \theta_2)$$

where $U = \{(\theta_1, \theta_2) \in \mathbf{R}^2 : \xi(\theta_1, \theta_2) \in N, \theta_1, \theta_2 \notin \{0, \pi\}\}$.

The Jacobian matrix of G has the form of three columns

$$DG(\theta_1, \theta_2, x) = (x\partial_1\boldsymbol{\nu}_1 + (1-x)\partial_1\boldsymbol{\nu}_2, x\partial_2\boldsymbol{\nu}_1 + (1-x)\partial_2\boldsymbol{\nu}_2, \boldsymbol{\nu}_1 - \boldsymbol{\nu}_2)$$

where ∂_i denotes $\partial/\partial\theta_i$ for $i = 1, 2$, and we see that its determinant is a quadratic expression $Q(x)$ in x with coefficients smooth functions of (θ_1, θ_2) .

Proposition 4.3 For (θ_1, θ_2) belonging to an open dense subset $\tilde{U} \subset U$ the quadratic equation $Q(x) = 0$ has distinct real solutions $x = x_i(\theta_1, \theta_2), i = 1, 2$.

Proof. See Appendix. \square

Therefore, since the distinct roots of a quadratic polynomial vary smoothly with the coefficients, the singular set

$$\tilde{\Sigma}_G := \{(\theta_1, \theta_2, x) \in \tilde{U} : \det DG(\theta_1, \theta_2, x) = 0\}$$

of $G|\tilde{U}$ has two connected components (smooth 2-manifolds) $\tilde{\Sigma}_G^1, \tilde{\Sigma}_G^2$ parametrised by $(\theta_1, \theta_2) \mapsto (\theta_1, \theta_2, x_i(\theta_1, \theta_2))$ for $i = 1, 2$.

4.3.3 Characterisation of fold points

The condition for a point of $\sigma \in \tilde{\Sigma}_G$ to exhibit a fold singularity is that $DG(\sigma)$ have rank 2 (therefore kernel dimension 1) and that the kernel of $DG(\sigma)$ be transverse to $\tilde{\Sigma}_G$ at that point: see [1],[17],[18]. The rank condition is equivalent to the condition that σ be a regular zero of $\det DG$, that is $\text{grad det } DG(\sigma) \neq 0$, and the transversality condition then is that $h(\sigma) \neq 0$ where $h(\sigma)$ is the scalar product

$$h(\sigma) := w(\sigma) \cdot \text{grad det } DG(\sigma) \quad (4.29)$$

and $\ker DG(\sigma) = \text{span}\{w(\sigma)\}$.

Writing

$$\det DG(\theta_1, \theta_2, x) = q(x - x_1)(x - x_2) \quad (4.30)$$

with q, x_1, x_2 functions of θ_1, θ_2 , an elementary calculation shows that where $\sigma = (\theta_1, \theta_2, x_1)$ we have

$$\text{grad det } DG(\sigma) = q(x_2 - x_1)(\partial_1 x_1, \partial_2 x_1, -1) \quad (4.31)$$

and similarly for x_2 . Moreover, a candidate for $w(\sigma)$ is given by any nonzero column $\mathbf{a}(\sigma)$ of the adjugate matrix $\text{adj } DG(\sigma)$. Therefore without loss of generality the function h in (4.29) may be replaced on $\tilde{\Sigma}_G^i$ by h_i given by

$$h_i(\sigma) := \mathbf{a}(\sigma) \cdot (\partial_1 x_i, \partial_2 x_i, -1).$$

We thus arrive at the following criterion for fold points:

Proposition 4.4 The singular point $\sigma \in \tilde{\Sigma}_G^i, i = 1, 2$ is a fold point if and only if $h_i(\sigma) \neq 0$.

Remark. The adjugate of a 3×3 matrix of rank 2 itself has rank 1, so that each column is a scalar multiple of the same nonzero column. Therefore in selecting a candidate for $\ker DG(\sigma)$ as above it is important to ensure that this scalar factor (a real-valued function of (θ_1, θ_2)) is nonzero at σ .

4.3.4 Further degeneracy

Generically we expect the locus $h_i = 0$ (where Proposition 4.4 fails) to be a smooth 1-manifold $\tilde{\Sigma}_G^{i1}$ in $\tilde{\Sigma}_G^i$, for which the image under G is a *cuspidal ridge* in Π , with possible isolated *swallowtail points*. The latter more degenerate points occur where $\ker DG(\sigma)$, which for $\sigma \in \tilde{\Sigma}_G^{i1}$ is by definition tangent to $\tilde{\Sigma}_G^i$ since $h_i = 0$, is also (quadratically) tangent to $\tilde{\Sigma}_G^{i1}$ (see [1],[17],[18]). In Figure 4.1 we give a numerical illustration with the help of MAPLE showing part of a cuspidal ridge in the bifurcation set $G(\tilde{\Sigma}_G^1) \subset \Gamma^L \cap \Pi$ in Π . In Figure 4.2(a) we show the curve $\tilde{\Sigma}_G^{11}$ in $\tilde{\Sigma}_G^1$ (parametrised by (θ_1, θ_2)) together with the direction of $\ker DG(\sigma)$ at three points σ on $\tilde{\Sigma}_G^{11}$, while Figure 4.2(b) shows the corresponding cuspidal ridge and swallowtail structure in the bifurcation set $\Gamma^L \cap \Pi$.

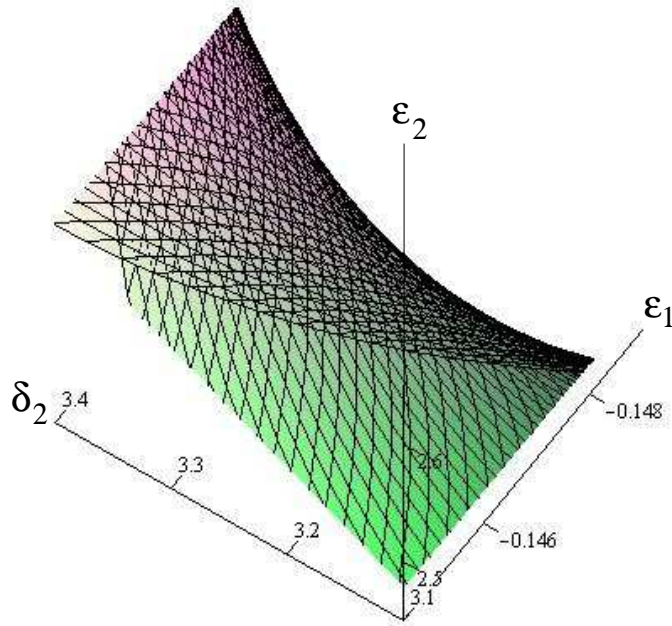


Figure 4.1: Part of a cuspidal ridge in the bifurcation set $\Gamma^L \cap \Pi$. The surface is more highly compressed than the figure suggests, lying close to the plane $\varepsilon_2 = 0.8 \delta_2$. Numerical parameter values are $c = 2/3$ and $\omega_2 = \eta \omega_1$ with $\eta = 2/5$ and such that $\omega_1^2 + \omega_2^2 = 2$ (so $\omega_1 = 1.1$, $\omega_2 = 0.88$ approx.), corresponding to $(c_1, c_2) \sim (0.14, 0.31)$. Detuning parameters are $\kappa_1 = 1, \kappa_2 = 2$.

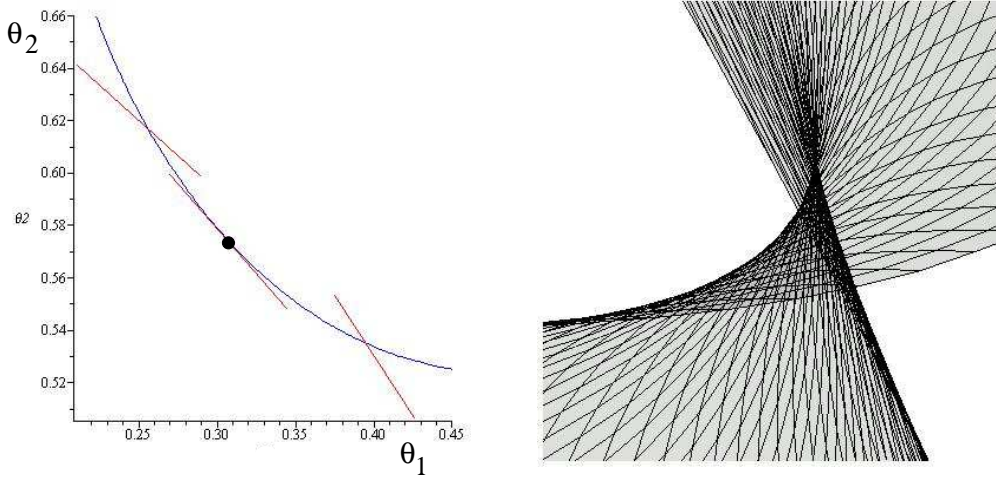


Figure 4.2: (a) A curve of cusp singular points for the map G , with an isolated swallowtail singular point where the kernel of DG is tangent to the cusp curve. (b) The corresponding swallowtail point in the plane Π at (approximately) $\varepsilon = (1, 2.94, -0.15, 2.40)$ in parameter space, showing the coalescence of two cusp ridges and (behind) the transverse intersection of two sheets of the fold surface. Parameter values as for Figure 4.1.

4.4 The full nonlinear problem

Recall that with the notation of Section 1.1.2

$$P_\varepsilon(\xi) = \rho \mathcal{P}(\xi)s + O(\rho^2) = \rho(\mathcal{P}(\xi)s + O(\rho))$$

for $\varepsilon = \rho s$ with $s \in S^3$. Solutions to $P_\varepsilon(\xi) = 0$ with $\varepsilon \neq 0$ and $|\varepsilon|$ small thus arise from the set M_1^L of solutions to the first order problem $\mathcal{P}(\xi)s = 0$ after applying a perturbation of $O(\rho)$ followed by rescaling by the factor ρ .

We have seen above that for every ξ in the open dense subset $\tilde{N} \subset N$, where

$$\tilde{N} := \{\xi(\theta_1, \theta_2) : (\theta_1, \theta_2) \in \tilde{U}\}$$

with \tilde{U} as in Proposition 4.3, there are two lines $L_1(\xi), L_2(\xi)$ through the origin in \mathbf{R}^4 such that

$$\{\xi\} \times (L_1(\xi) \cup L_2(\xi))$$

consists of singular points of the projection $N^L \rightarrow \mathbf{R}^4$, and the part of the singular set Ξ^L that corresponds to \tilde{N} is precisely the union of these lines as ξ runs through \tilde{N} . Each line $L_i(\xi)$ intersects the unit sphere S^3 in an antipodal pair of points $\ell_i^\pm(\xi)$ which (when $\varepsilon_1 \neq 0$) are the radial projections

from Π of the point $G(\theta_1, \theta_2, x_i(\theta_1, \theta_2))$. The points $\{\xi\} \times \{\ell_i^\pm\}$ are singular points of the projection $N_1^L \rightarrow S^3$.

At these points the projection $N_1^L \rightarrow S^3$ typically exhibits a fold singularity, so that locally there is a smooth 2-dimensional *fold surface* K_1^L in S^3 such that the number of solutions $\xi \in N$ to the first-order problem $\mathcal{P}(\xi)\varepsilon = 0$ changes by two as ε crosses K_1^L . The stability of fold singularities under C^∞ perturbations implies that for sufficiently small $\rho > 0$ the same holds for the nonlinear problem $P_\varepsilon(\xi) = 0$ with $|\varepsilon| = \rho$. To be precise, let us write

$$\tilde{N}_\rho := M \cap (\tilde{N} \times \rho S^3), \quad \tilde{N}_\rho^L := M^L \cap (\tilde{N} \times \rho S^3).$$

Then the projection $pr : \rho^{-1}\tilde{N}_\rho \rightarrow S^3$ has a corresponding fold obtained from that of $pr : \rho^{-1}\tilde{N}_\rho^L = \tilde{N}_1^L \rightarrow S^3$ by a local C^∞ diffeomorphism close to the identity and tending to the identity as $\rho \rightarrow 0$. (Here the rescaling ρ^{-1} is understood to apply in the second (that is ε) component only.) Hence for sufficiently small $\rho > 0$ the projection $\tilde{N}_\rho \rightarrow \rho S^3$ itself exhibits a fold with fold surface $K_\rho \subset \rho S^3$, so that the number of solutions $\xi \in N$ to $P_\varepsilon(\xi) = 0$ changes by two as ε crosses K_ρ in ρS^3 . The local fold bifurcation set for the first order problem is a cone K^L from the origin in \mathbf{R}^4 to the local fold surface K_1^L in S^3 , and so this corresponds to a ‘curved’ cone structure for the bifurcation set for the nonlinear problem: the ‘curved’ cone K is obtained from K^L by applying a diffeomorphism¹ at the origin in \mathbf{R}^4 with derivative the identity.

Fold surfaces for $N_1^L \rightarrow S^3$ meet in cusp ridges, corresponding to points $\xi \in N$ that are regular zeros of the function $h_i(\xi, x_i(\xi))$ for $i = 1$ or 2 . As above, these give rise to cones on cusp ridges for the bifurcation set of the first order problem, and ‘curved’ cones on cusp ridges for the nonlinear problem with $\rho > 0$ sufficiently small. Likewise, isolated swallowtail points for $N_1^L \rightarrow S^3$ correspond to C^∞ arcs through the origin (C^1 at the origin) of swallowtail bifurcation points for the nonlinear problem. For sufficiently small $\rho > 0$ the overall configuration of curved cones on fold surfaces, cusp ridges and swallowtail points constitutes the bifurcation set Γ for the nonlinear problem $P_\varepsilon(\xi) = 0$.

We have not verified explicitly that the functions $h_i : \tilde{\Sigma}_G \rightarrow \mathbf{R}, i = 1, 2$ do satisfy the generic conditions needed to ensure the C^∞ stability of the cusp ridges and swallowtail points of the projection $\tilde{N}_1^L \rightarrow S^3$, or (equivalently) that the line congruence $\mathcal{A} \cap \Pi$ satisfies the generic conditions in [22]. Nevertheless, numerical evidence indicates (as would be expected) that at least

¹This diffeomorphism is C^∞ away from the origin, but may be only C^1 at the origin itself.

for an open dense set of coefficients c_1, c_2 in (4.1) and detuning parameters κ_1, κ_2 in (4.14) this is indeed the case.

4.5 Interpretation of the bifurcation geometry

We conclude by recalling how the bifurcation geometry described above relates to the original problem of persistence of periodic solutions of period close to T for a pair of coupled van der Pol oscillators (4.1). Recall that here $T = m \frac{2\pi}{\omega_1} = n \frac{2\pi}{\omega_2}$ and for simplicity (see Section 4.1) we assume $m \neq 3n$.

As $\varepsilon = (\delta_1, \delta_2, \varepsilon_1, \varepsilon_2)$ traces out a smooth path close to (but not passing through) the origin in parameter space \mathbf{R}^4 there exists a corresponding finite set of solutions ξ to the equation $P_\varepsilon(\xi) = 0$ close to the 2-dimensional manifold \tilde{N} (an open dense subset of a torus) in phase space \mathbf{R}^4 . These are fixed points of the map F_ε , and correspond to T' -periodic solutions (T' close to T) with initial data ξ of the non-autonomous perturbed coupled van der Pol system (4.1). A typical path in \mathbf{R}^4 will intersect the bifurcation set Γ ('curved' cone) transversely at discrete points ε which correspond to the creation or annihilation of pairs of periodic orbits in saddle-node (fold) bifurcations. For any given $\xi \in \tilde{N}$ there exists $\rho_0 > 0$ such that there exist two C^1 curves $\gamma_1(\xi), \gamma_2(\xi)$ through the origin in parameter space \mathbf{R}^4 , tangent at the origin to the lines $\{L_1(\xi), L_2(\xi)\}$ as described in Section 4.3, such that a saddle-node bifurcation occurs close to ξ in phase space \mathbf{R}^4 whenever ε passes through $\gamma_1(\xi)$ or $\gamma_2(\xi)$ and $|\varepsilon| < \rho_0$. The point in phase space at which the bifurcation occurs tends to ξ as $\rho \rightarrow 0$.

Paths in bifurcation space \mathbf{R}^4 will typically avoid the 2-dimensional curved cones on cusp ridges and any isolated swallowtail arcs, but 2-parameter families in \mathbf{R}^4 close to the origin will typically encounter isolated parameter values corresponding to cusp bifurcations of T' -periodic orbits, while 3-parameter families will typically encounter swallowtails. Note that a swallowtail bifurcation point lies on a C^1 curve of swallowtail points through the origin in parameter space, and corresponds to a point $\xi \in \tilde{N}$ from which *four* T' -periodic orbits may simultaneously bifurcate.

Remark. A path $\varepsilon(\tau)$ in \mathbf{R}^4 with $\varepsilon(\tau) \rightarrow 0 \in \mathbf{R}^4$ as $\tau \rightarrow \tau_0$ need not correspond to a path of solutions $\xi(\tau)$ to $P_\varepsilon(\xi) = 0$ approaching a point $(\xi, 0)$ in the solution locus M . For this to be the case we require $\varepsilon(\tau)/|\varepsilon(\tau)|$ to tend to a limit in S^3 as $\tau \rightarrow \tau_0$. See [20] for further discussion of this important point.

In this analysis we have not discussed stability of bifurcating periodic orbits. An argument similar to that of Section 3.5 for a single oscillator shows

that stability is determined by the eigenvalues of the matrix $L(\xi, \varepsilon)$ as in the Appendix below. We have also not attempted here to give a complete description of the global bifurcation behaviour in terms of the full 4-dimensional geometry and the structure of the associated line congruence of singularities. The remainder of this task as well as the stability analysis is left to the enthusiastic reader.

5 Appendix: specific calculations

In this Appendix we look more closely at the structure of the singular set of the projection $pr|N^L : N^L \rightarrow \mathbf{R}^4$. With the parametrization Φ from (4.27) the singular set of $pr|N^L$ corresponds to that of the map $\mathbf{R}^4 \rightarrow \mathbf{R}^4$ given by

$$(\theta_1, \theta_2, x, y) \mapsto x\boldsymbol{\mu}_1(\theta_1, \theta_2) + y\boldsymbol{\mu}_2(\theta_1, \theta_2).$$

We have seen in Section 4.3 that the IFT implies that this projection map can be singular only where (for given $\varepsilon \in \mathbf{R}^4$) the map $\Psi : \mathbf{R}^4 \rightarrow \mathbf{R}^4 : \xi \mapsto \mathcal{P}(\xi)\varepsilon$ is singular. Let us denote the derivative of Ψ at (ξ, ε) by $L = L(\xi, \varepsilon)$.

Recall that for $\xi \in N$ the first two rows of the matrix $\mathcal{P}(\xi)$ are identically zero, and so the kernel of $\mathcal{P}(\xi)$ is the kernel of the 2×4 matrix $A(\xi)$ of rank 2, where

$$A(\xi) = \begin{pmatrix} \omega_1^{-1}p_1 & \omega_1^{-1}q_1 & a_1 \sin \theta_1 & 0 \\ \omega_2^{-1}p_2 & \omega_2^{-1}q_2 & 0 & -a_2c \sin \theta_2 \end{pmatrix}. \quad (5.1)$$

This enables us to simplify the description of L .

Lemma 5.1 *Let $\xi \in N$ and $\varepsilon \in \mathbf{R}^4$ such that $\varepsilon \in \ker \mathcal{P}(\xi)$. The linear map $L : \mathbf{R}^4 \rightarrow \mathbf{R}^4$ is singular if and only if $\det Q(\xi, \varepsilon) = 0$ where*

$$Q(\xi, \varepsilon) = \begin{pmatrix} q_{11}(\xi, \varepsilon) & q_{12}(\xi, \varepsilon) \\ q_{21}(\xi, \varepsilon) & q_{22}(\xi, \varepsilon) \end{pmatrix}$$

with $q_{ij}(\xi, \varepsilon) = \varepsilon^\dagger \partial \mathbf{a}_i / \partial \theta_j$ in which \mathbf{a}_i^\dagger is the i^{th} row of the matrix $A(\xi)$ for $i = 1, 2$, and where $\xi \in N$ is parametrised as $\xi(\theta_1, \theta_2)$ using (4.24) and (4.25).

Proof. This proceeds by analogy with the proof of Lemma 3.6. Writing

$$\mathcal{P}(\xi) \varepsilon = \begin{pmatrix} \mathbf{v} \\ \mathbf{w} \end{pmatrix}$$

with $\mathbf{v}, \mathbf{w} \in \mathbf{R}^2$ and using polar coordinates $(r_1, r_2, \theta_1, \theta_2)$ in the domain of L we have

$$L = \begin{pmatrix} \mathbf{v}_r & \mathbf{v}_\theta \\ \mathbf{w}_r & \mathbf{w}_\theta \end{pmatrix}$$

where \mathbf{v}_r denotes the 2×2 matrix with columns $\frac{\partial \mathbf{v}}{\partial r_1}, \frac{\partial \mathbf{v}}{\partial r_2}$ and so on. Then by analogy with (3.8) at points of N

$$L \begin{pmatrix} \mathbf{r}'(\theta) \\ I \end{pmatrix} = \begin{pmatrix} \mathbf{v}'(\theta) \\ \mathbf{w}'(\theta) \end{pmatrix} = \begin{pmatrix} 0 \\ \mathbf{w}'(\theta) \end{pmatrix} \quad (5.2)$$

since $\mathbf{v} = 0$ identically on N . Here $\mathbf{r}'(\theta)$ denotes the 2×2 Jacobian matrix of $\mathbf{r} = (r_1, r_2)$ with respect to $\theta = (\theta_1, \theta_2)$ where N is parametrised by $\mathbf{r} = \mathbf{r}(\theta)$ as in (4.25), while $\mathbf{v}'(\theta), \mathbf{w}'(\theta)$ are the Jacobian matrices of \mathbf{v}, \mathbf{w} with respect to (θ_1, θ_2) after the substitutions (4.25), and I is the 2×2 identity matrix. It is easy to check that \mathbf{v}_r is invertible, and then applying the invertible 4×4 matrix

$$J := \begin{pmatrix} I & 0 \\ -\mathbf{w}_r \mathbf{v}_r^{-1} & I \end{pmatrix}$$

to both sides of (5.2) gives

$$\begin{pmatrix} \mathbf{v}_r & \mathbf{v}_\theta \\ 0 & \mathbf{w}_\theta - \mathbf{w}_r \mathbf{v}_r^{-1} \mathbf{v}_\theta \end{pmatrix} \begin{pmatrix} \mathbf{r}'(\theta) \\ I \end{pmatrix} = \begin{pmatrix} 0 \\ \mathbf{w}'(\theta) \end{pmatrix} \quad (5.3)$$

from which since $\det J = 1$ it follows that

$$\det L = \det JL \quad (5.4)$$

$$= \det \mathbf{v}_r \det(\mathbf{w}_\theta - \mathbf{w}_r \mathbf{v}_r^{-1} \mathbf{v}_\theta) \quad (5.5)$$

$$= \det \mathbf{v}_r \det \mathbf{w}'(\theta). \quad (5.6)$$

Therefore L is invertible if and only if $\mathbf{w}'(\theta)$ is invertible. However, $\mathbf{w}'(\theta)$ is precisely the matrix $Q(\xi, \varepsilon)$ as in the statement of the Lemma. \square

After substitution $\varepsilon = x\boldsymbol{\mu}_1 + y\boldsymbol{\mu}_2$ the determinant of $Q(\xi, \varepsilon)$ becomes a quadratic form in (x, y) with coefficients depending on $\xi \in N$:

$$\det Q(\xi, \varepsilon) = \mathcal{Q}(\xi)(x, y). \quad (5.7)$$

In general we might expect there to be nonempty open sets in N where $\mathcal{Q}(\xi)$ is definite and where it is indefinite. However, we now show that in fact the quadratic form $\mathcal{Q}(\xi)$ is never definite, so that Proposition 4.3 holds.

To find the entries q_{ij} in the matrix Q of Lemma 5.1 we calculate explicitly the partial derivatives $m_{ij} := \partial \mathbf{a}_i / \partial \theta_j$ and find

$$m_{11} = 8t_1^2 \omega_1^{-1} \sin \theta_1 \cos \theta_1 (1, d^2, 0, 0)^\dagger + 2t_1^{-1} (\omega_1 \cos \theta_1)^{-2} (0, 0, 1, 0)^\dagger$$

$$m_{12} = 16t_2^2 \omega_1^{-1} \sin \theta_2 \cos \theta_2 (1, d^2, 0, 0)^\dagger$$

$$m_{21} = 16t_1^2 \omega_2^{-1} \sin \theta_1 \cos \theta_1 (1, d^2, 0, 0)^\dagger$$

$$m_{22} = 8t_2^2 \omega_2^{-1} \sin \theta_2 \cos \theta_2 (1, d^2, 0, 0)^\dagger + 2ct_2^{-1} (\omega_2 \cos \theta_2)^{-2} (0, 0, 0, 1)^\dagger.$$

Substituting $\varepsilon = \boldsymbol{\mu}_1$ and $\varepsilon = \boldsymbol{\mu}_2$ in turn into $q_{ij} = \varepsilon^t m_{ij}$ we obtain two 2×2 matrices $Q_1(\xi), Q_2(\xi)$ where

$$Q_1 = -32t_1(d^2 - 1)\omega_1^{-3} \begin{pmatrix} 2 \sin^2 \theta_1 - 1 + t_{21}^2 c_{21}^2 & 4t_{21}^2 c_{21} \sin \theta_1 \sin \theta_2 \\ 4\omega_{12} \sin^2 \theta_1 & 2\omega_{12} t_{21}^2 c_{21} \sin \theta_1 \sin \theta_2 \end{pmatrix}, \quad (5.8)$$

$$Q_2 = -32ct_2(d^2 - 1)\omega_2^{-3} \begin{pmatrix} 2\omega_{21} t_{12}^2 c_{12} \sin \theta_1 \sin \theta_2 & 4\omega_{21} \sin^2 \theta_2 \\ 4t_{12}^2 c_{12} \sin \theta_1 \sin \theta_2 & 2 \sin^2 \theta_2 - 1 + t_{12}^2 c_{12}^2 \end{pmatrix} \quad (5.9)$$

in which

$$\begin{aligned} \omega_{12} &= \frac{\omega_1}{\omega_2} = \omega_{21}^{-1} \\ t_{12} &= \frac{t_1}{t_2} = t_{21}^{-1} = d\omega_{21}^3 \frac{\kappa_2}{\kappa_1} \\ c_{12} &= \frac{\cos \theta_1}{\cos \theta_2} = c_{21}^{-1}. \end{aligned}$$

Observe the symmetry: Q_2 is obtained from Q_1 by interchanging suffices 1 and 2 apart from the factor c . This is of course a consequence of the symmetry of the original system (4.1) and the slight asymmetry in the choice of the diagonalisation matrix (4.2). Note also that t_{12} is inversely proportional to the detuning coefficient ratio κ_1/κ_2 .

We are now in a position to calculate the quadratic form $\mathcal{Q}(\xi)$ in (5.7). We have

$$\mathcal{Q}(\xi)(x, y) = \det(xQ_1(\xi) + yQ_2(\xi)) \quad (5.10)$$

$$= D_{11}x^2 + (D_{12} + D_{21})xy + D_{22}y^2 \quad (5.11)$$

where D_{ij} is the determinant of the 2×2 matrix whose first column is that of Q_i and second column is that of Q_j for $i, j \in \{1, 2\}$. The discriminant of $\mathcal{Q}(\xi)$ is

$$\Delta_{\mathcal{Q}} := (D_{12} + D_{21})^2 - 4D_{11}D_{22}.$$

After some algebra in which agreeable cancellations occur, we arrive at the following result.

Proposition 5.2 *Up to multiplication by a positive constant*

$$\Delta_{\mathcal{Q}} = (A_1 s_1^2 + A_2 s_2^2 + \frac{1}{2} A_1 A_2)^2 - 16A_1 A_2 s_1^2 s_2^2$$

where $s_i = \sin \theta_i$ ($i = 1, 2$) and $A_1 = t_{12}^2 c_{12}^2 - 1$, $A_2 = t_{21}^2 c_{21}^2 - 1$; note that $A_1 A_2 = -(A_1 + A_2)$. \square

It can easily be checked that $A_1 A_2 \leq 0$ with equality if and only if $A_1 = A_2 = 0$, that is

$$t_1 \cos \theta_1 = t_2 \cos \theta_2 \quad \text{i.e. } r_1 = r_2. \quad (5.12)$$

As an easy consequence we conclude the following.

Proposition 5.3 *The discriminant $\Delta_{\mathcal{Q}} \geq 0$ for all (θ_1, θ_2) , with $\Delta_{\mathcal{Q}} = 0$ if and only if either (5.12) holds or θ_1, θ_2 satisfy one or other of the two conditions*

$$\begin{aligned} s_1 = 0, \quad (1 - s_2^2)(1 - 2s_2^2) &= t_{12}^2 & \text{or} \\ s_2 = 0, \quad (1 - s_1^2)(1 - 2s_1^2) &= t_{21}^2. \end{aligned}$$

□

Let $\tilde{U} \subset U$ be the dense open subset on which none of these equations is satisfied, so that $\Delta_{\mathcal{Q}} > 0$ for $(\theta_1, \theta_2) \in \tilde{U}$, and let \tilde{N} be the corresponding open dense subset of N .

Corollary 5.4 *For all $\xi \in \tilde{N}$ the quadratic form $\mathcal{Q}(\xi)(x, y)$ is nondegenerate and indefinite.* □

Consequently every $\xi \in \tilde{N}$ is a potential fold bifurcation point from which a pair of T' -periodic orbits of (1.1), mutually annihilating or appearing, may emanate as $\varepsilon = (\delta_1, \delta_2, \varepsilon_1, \varepsilon_2)$ moves away from the origin in \mathbf{R}^4 in an appropriate direction (one of two directions, and their negatives). To decide if ξ corresponds to a more degenerate cusp ridge point (three T' -periodic points coinciding) or a swallowtail point (four T' -periodic points) requires evaluating the functions h_1, h_2 as in Proposition 4.4, as well as the alignment of $\ker DG(\sigma)$ at the corresponding points σ of the singularity set $\tilde{\Sigma}_G$ as described in Section 4.4.

References

- [1] V. I. ARNOLD, *Singularities of smooth mappings*, Russian Math. Surveys 23 (1968), pp. 1–43.
- [2] V. I. ARNOLD, *Lectures on bifurcations in versal families*, Russian Math. Surveys 27 (1972), pp. 119–184.
- [3] V. I. ARNOLD, *Geometrical Methods in the Theory of Ordinary Differential Equations*, Springer 1983.

- [4] D.G. ARONSON, G.B. ERMENTROUT AND N. KOPELL, *Amplitude response of coupled oscillators*, Physica D 41 (1990), pp. 403–449.
- [5] C. BAESENS, J. GUCKENHEIMER, S. KIM AND R. S. MACKAY, *Three coupled oscillators: mode-locking, global bifurcations and toroidal chaos*, Physica D 49 (1991), pp. 387–475.
- [6] E. CAMACHO, R. RAND AND H. HOWLAND, *Dynamics of two van der Pol oscillators coupled via a bath*, Int. J. Solids and Structures 41 (2004), pp. 2133–2143.
- [7] C. CHICONE, *Lyapunov-Schmidt reduction and Melnikov integrals for bifurcation of periodic solutions in coupled oscillators*, J. Diff. Eqns 112 (1994), pp. 407–447.
- [8] C. CHICONE, *Bifurcations of nonlinear oscillations and frequency entrainment near resonance*, SIAM J. Math. Anal. 23 (1992), pp. 1577–1608.
- [9] C. CHICONE, *Periodic solutions of a system of coupled oscillators near resonance*, SIAM J. Math. Anal. 26 (1995), pp. 1257–1283.
- [10] C. CHICONE, *A geometric approach to regular perturbation theory with an application to hydrodynamics*, Trans. Amer. Math. Soc. 347 (1995), pp. 4559–4598.
- [11] D. R. J. CHILLINGWORTH, *Generic multiparameter bifurcation from a manifold*, Dynamics and Stability of Systems 15 (2000), pp. 101–137.
- [12] S.-N. CHOW AND J. K. HALE, *Methods of Bifurcation Theory*, Springer 1982.
- [13] E. A. CODDINGTON AND N. LEVINSON, *Theory of Ordinary Differential Equations*, McGraw-Hill 1955.
- [14] S. P. DILIBERTO, *On systems of ordinary differential equations*, in Contributions to the Theory of Nonlinear Oscillations, Ann. Math. Studies Vol. 20, Princeton University Press 1950.
- [15] K. S. FINK, G. JOHNSON, T. CARROLL, D. MAR AND L. PECORA, *Three coupled oscillators as a universal probe of synchronization stability in coupled oscillator arrays*, Phys. Rev. E 61 (2000), pp. 5080–5090.

- [16] G. GENTILE, M. BARTUCELLI AND J. DEANE, *Bifurcation curves of subharmonic solutions and Melnikov theory under degeneracies*, Rev. Math. Phys. 19 (2007), pp. 307–348.
- [17] C. G. GIBSON, *Singular Points of Smooth Mappings*, Res. Notes in Math. 25, Pitman, 1979.
- [18] M. GOLUBITSKY AND V. GUILLEMIN, *Stable Mappings and their Singularities*, Springer, 1973.
- [19] J. GUCKENHEIMER AND P. HOLMES, *Nonlinear Oscillations, Dynamical Systems, and Bifurcations of Vector Fields*, Springer, 1983.
- [20] J. K. HALE AND P. Z. TABOAS, *Interaction of damping and forcing in a second order equation*, Nonlinear Anal. 2 (1978), pp. 77–84.
- [21] M.V. IVANCHENKO, G.V. OSIPOV, V.D. SHALFEEV AND J. KURTHS, *Synchronization of two non-scalar-coupled limit-cycle oscillators*, Physica D 189 (2004), pp. 8–30.
- [22] S. IZUMIYA, K. SAJI AND N. TAKEUCHI, *Singularities of line congruences*, Proc. Roy. Soc. Edinburgh 133A (2003), pp. 1341–1359.
- [23] M. I. KAMENSKII, O. YU. MAKARENKO AND P. NISTRI *A new approach to the theory of ordinary differential equations with a small parameter*, Doklady Math. 67 (2003), pp. 439–442.
- [24] A. P. KUZNETSOV AND J. P. ROMAN, *Properties of synchronization in the systems of non-identical coupled van der Pol and van der Pol – Duffing oscillators. Broadband synchronization*, Physica D 238 (2009), pp. 1499–1506.
- [25] S. LEFSCHETZ, *Differential Equations: Geometric Theory*, 2nd ed., Dover, New York, 1977.
- [26] N. MINORSKY, *Nonlinear Oscillations*, Van Nostrand, New York, 1962.
- [27] R. H. RAND AND P. J. HOLMES, *Bifurcation of periodic motions in two weakly coupled Van Der Pol oscillators*, Int. J. Non-Linear Mechanics 15 (1980), pp. 387–399.
- [28] K. ROMPALA, R. RAND AND H. HOWLAND, *Dynamics of three coupled van der Pol oscillators with application to circadian rhythms*, Comm. Nonlin. Sci. Numer. Simulation 12 (2007), pp. 794–803.

- [29] S. H. STROGATZ AND I. STEWART, *Coupled oscillators and biological synchronization*, Nature 269 (1993), pp. 102–109.
- [30] R. THOM, *Structural Stability and Morphogenesis*, W.A.Benjamin, 1975.